

## HELPER T CELLS

Human “T<sub>H</sub>9” cells are a subpopulation of PPAR- $\gamma$ <sup>+</sup> T<sub>H</sub>2 cells

Claire Micossé<sup>1\*</sup>, Leonhard von Meyenn<sup>1\*</sup>, Oliver Steck<sup>1</sup>, Enja Kipfer<sup>1</sup>, Christian Adam<sup>2</sup>, Cedric Simillion<sup>3</sup>, S. Morteza Seyed Jafari<sup>1</sup>, Peter Olah<sup>4</sup>, Nikhil Yawalkar<sup>1</sup>, Dagmar Simon<sup>1</sup>, Luca Borradori<sup>1</sup>, Stefan Kuchen<sup>5</sup>, Daniel Yerly<sup>5</sup>, Bernhard Homey<sup>4</sup>, Curdin Conrad<sup>6</sup>, Berend Snijder<sup>7</sup>, Marc Schmidt<sup>2</sup>, Christoph Schlapbach<sup>1†</sup>

Although T<sub>H</sub>1, T<sub>H</sub>2, and T<sub>H</sub>17 cells are well-defined T<sub>H</sub> cell lineages in humans, it remains debated whether IL-9-producing T<sub>H</sub> cells represent a bona fide “T<sub>H</sub>9” lineage. Our understanding of the cellular characteristics and functions of IL-9-producing T<sub>H</sub> cells in humans is still nascent. Here, we report that human IL-9-producing T<sub>H</sub> cells express the chemokine receptors CCR4 and CCR8, produce high levels of IL-5 and IL-13, and express T<sub>H</sub>2 lineage-associated transcription factors. In these cells, IL-9 production is activation dependent, transient, and accompanied by down-regulation of T<sub>H</sub>2 cytokines, leading to an apparent “T<sub>H</sub>9” phenotype. IL-9<sup>+</sup> T<sub>H</sub>2 cells can be distinguished from “conventional” T<sub>H</sub>2 cells based on their expression of the transcription factor PPAR- $\gamma$ . Accordingly, PPAR- $\gamma$  is induced in naïve T<sub>H</sub> cells by priming with IL-4 and TGF- $\beta$  (“T<sub>H</sub>9” priming) and is required for IL-9 production. In line with their identity as early activated T<sub>H</sub>2 cells, IL-9<sup>+</sup> T<sub>H</sub>2 cells are found in acute allergic skin inflammation in humans. We propose that IL-9-producing T<sub>H</sub> cells are a phenotypically and functionally distinct subpopulation of T<sub>H</sub>2 cells that depend on PPAR- $\gamma$  for full effector functions.

## INTRODUCTION

T helper (T<sub>H</sub>) cells are crucial mediators of the immune system and have evolved into specialized subsets to orchestrate specific types of immune responses. Among the proinflammatory effector T<sub>H</sub> cell subsets, T<sub>H</sub>1, T<sub>H</sub>2, and T<sub>H</sub>17 cells have been identified as discrete subsets with distinct phenotypic and functional properties (1, 2). Interleukin-9 (IL-9)-producing “T<sub>H</sub>9” cells have been proposed as a new T<sub>H</sub> subset because they were found to express IL-9 in the absence of coexpression of subset-defining cytokines and transcription factors (3, 4). However, the existence of a bona fide “T<sub>H</sub>9” lineage has not been proven, and the relevance of “T<sub>H</sub>9” cells in humans remains to be elucidated. A T cell lineage is defined as a population of T cells in which a distinct cytokine profile is induced by polarizing signals and genetically regulated by lineage-specifying transcription factors (5). For instance, T<sub>H</sub>2 cells are differentiated under the influence of IL-4 and require the transcription factor GATA3 for stable induction of IL-4, IL-5, and IL-13 (6). Furthermore, T<sub>H</sub> cell subsets also express distinct chemokine receptor profiles. T<sub>H</sub>17 cells, for example, all express CCR6, whereas CXCR3 and CCR4 primarily identify T<sub>H</sub>1 or T<sub>H</sub>2 cells, respectively (1, 7, 8). Each T<sub>H</sub> cell lineage can thus be defined by distinct polarization requirements as well as the expression of subset-specific cytokines, transcription factors, and chemokine receptors.

Before “T<sub>H</sub>9” cells can be considered a distinct T<sub>H</sub> cell subset, key lineage-defining properties of IL-9-expressing T<sub>H</sub> cells need to be defined. Unequivocal data showing that IL-9-producing T<sub>H</sub> cells are distinct from already defined T<sub>H</sub> cell subsets are lacking. This is likely the consequence of the transient and activation-dependent

expression kinetics of IL-9 in T<sub>H</sub> cells seen in vitro (9), in disease models (10–12), and in vivo (13, 14). In humans, the “T<sub>H</sub>9” phenotype—defined as IL-9 expression in the absence of coexpression of signature T<sub>H</sub> subset cytokines or transcription factors—has so far only been observed after activation of in vitro-primed naïve T<sub>H</sub> cells or of skin-homing memory T<sub>H</sub> cells (9). However, the cellular identity of these IL-9-producing cells before they up-regulate IL-9 and after they have down-regulated IL-9 is not known. Further, a lineage-defining transcription factor for “T<sub>H</sub>9” cells still awaits identification (15). Last, a specific chemokine receptor profile of “T<sub>H</sub>9” cells has not been described. Together, a precise definition of “T<sub>H</sub>9” cells that would allow to differentiate them from other T<sub>H</sub> cell subsets with the ability to secrete IL-9 is missing.

We therefore sought to explore whether “T<sub>H</sub>9” cells represent a distinct human T<sub>H</sub> cell subset by comprehensively characterizing the lineage-defining properties of human IL-9-expressing T<sub>H</sub> cells. We performed ex vivo analysis of IL-9-expressing T<sub>H</sub> cells and defined their chemokine receptor profile, their cytokine profile, and their transcription factors irrespective of activation status. These results were compared with the properties of in vitro-primed “T<sub>H</sub>9” cells. Last, we investigated the role of IL-9-expressing T<sub>H</sub> cells in human skin inflammation. We found that in this setting, IL-9-expressing T<sub>H</sub> cells are a subpopulation of T<sub>H</sub>2 cells that show activation-dependent cytokine profiles that give rise to a “T<sub>H</sub>9” phenotype. IL-9<sup>+</sup> T<sub>H</sub>2 cells produce high levels of IL-5 and IL-13 in the resting state, are enriched in the CCR4<sup>+</sup>/CCR8<sup>+</sup> population of effector memory T<sub>H</sub> cells, and express high levels of the transcription factor peroxisome proliferator-activated receptor- $\gamma$  (PPAR- $\gamma$ ), which, in turn, regulates IL-9 expression.

## RESULTS

IL-9-expressing T<sub>H</sub> cells are CCR4<sup>+</sup>/CCR8<sup>+</sup> effector memory T<sub>H</sub> cells

Resting T<sub>H</sub> cells do not produce IL-9, but a subset of memory T<sub>H</sub> cells transiently adopt a “T<sub>H</sub>9” phenotype after T cell receptor (TCR)

<sup>1</sup>Department of Dermatology, Inselspital, Bern University Hospital, University of Bern, Bern, Switzerland. <sup>2</sup>Department of Dermatology, University Hospital Würzburg, Würzburg, Germany. <sup>3</sup>Interfaculty Bioinformatics Unit and SIB Swiss Institute of Bioinformatics, University of Bern, Bern, Switzerland. <sup>4</sup>Department of Dermatology, University Hospital Düsseldorf, Düsseldorf, Germany. <sup>5</sup>Department of Rheumatology, Immunology and Allergology, Bern University Hospital, University of Bern, Bern, Switzerland. <sup>6</sup>Department of Dermatology, University Hospital CHUV, Lausanne, Switzerland. <sup>7</sup>Institute of Molecular Systems Biology, ETH, Zurich, Switzerland.

\*These authors contributed equally to this work.

†Corresponding author. Email: christoph.schlapbach@insel.ch

activation (9, 16). To identify their cellular identity, we performed time course analyses of their cytokine expression before and after activation. First, the differentiation status and phenotypic stability of IL-9-expressing T<sub>H</sub> cells were analyzed. We sorted naïve, central memory (T<sub>CM</sub>), and effector memory T (T<sub>EM</sub>) cells and tested their ability to produce IL-9 after activation (Fig. 1A). IL-9 was expressed in T<sub>EM</sub> cells, but not in naïve T<sub>H</sub> or T<sub>CM</sub> cells. In T<sub>EM</sub> cells, repeated rounds of activation lead to recurring waves of IL-9 expression (Fig. 1B). We concluded that transient IL-9 expression after activation is an intrinsic property of a subpopulation of CD4<sup>+</sup> T<sub>EM</sub> cells.

To determine the chemokine receptor profile of “T<sub>H9</sub>” cells, we sorted memory T<sub>H</sub> cells based on the expression of chemokine receptors known to be differentially expressed on T<sub>H</sub> cell subsets and assessed the frequency of cells with a “T<sub>H9</sub>” phenotype (“IL-9<sup>single+</sup>” = IL-9<sup>+</sup>/IFN-γ<sup>-</sup>/IL-13<sup>-</sup>/IL-17<sup>-</sup>) after activation (Fig. 1, C and D). “T<sub>H9</sub>” cells were significantly enriched in CXCR3<sup>-</sup>, CCR4<sup>+</sup>, CCR6<sup>-</sup>, and CCR8<sup>+</sup> T<sub>H</sub> cells, respectively. CCR8<sup>+</sup> T<sub>H</sub> cells were found to represent a subset of CXCR3<sup>-</sup>/CCR4<sup>+</sup>/CCR6<sup>-</sup> cells (Fig. 1E) that contained most IL-9<sup>single+</sup> cells (Fig. 1, F and H). Thus, T<sub>H</sub> cells that adopt the “T<sub>H9</sub>” phenotype share the chemokine receptor profile with T<sub>H2</sub> cells (CXCR3<sup>-</sup>/CCR4<sup>+</sup>/CCR6<sup>-</sup>) but express the skin-homing receptor CCR8 (1, 9, 17). Six days after activation, CXCR3<sup>-</sup>/CCR6<sup>-</sup>/CCR4<sup>+</sup>/CCR8<sup>+</sup> T<sub>H</sub> cells had down-regulated IL-9 but expressed high levels of IL-5 and IL-13 (Fig. 1, G and H). Collectively, the above results showed that IL-9<sup>+</sup> T<sub>H</sub> cells are a discrete subpopulation of CCR4<sup>+</sup>/CCR8<sup>+</sup> T<sub>H</sub> cells that share characteristics of T<sub>H2</sub> cells.

### T<sub>H</sub> cells that express IL-9 after activation express high levels of T<sub>H2</sub> cytokines in the resting state

To understand the origin and fate of IL-9-expressing T<sub>H</sub> cells at the single-cell level, we generated clones from ex vivo-isolated memory T<sub>H</sub> cells that were sorted on the basis of chemokine receptor expression (fig. S1A): T<sub>H1</sub> (“CXCR3<sup>+</sup>” = CXCR3<sup>+</sup>/CCR4<sup>-</sup>/CCR6<sup>-</sup>), T<sub>H17</sub> (“CCR6<sup>+</sup>” = CXCR3<sup>-</sup>/CCR4<sup>+</sup>/CCR6<sup>+</sup>), T<sub>H2</sub> (“CCR4<sup>+</sup>/CCR8<sup>-</sup>” = CXCR3<sup>-</sup>/CCR4<sup>+</sup>/CCR6<sup>-</sup>/CCR8<sup>-</sup>), and “T<sub>H9</sub>” (“CCR4<sup>+</sup>/CCR8<sup>+</sup>” = CXCR3<sup>-</sup>/CCR4<sup>+</sup>/CCR6<sup>-</sup>/CCR8<sup>+</sup>). The cytokine profile of these clones was then analyzed before and after activation (Fig. 2 and fig. S1B). We found that IL-9 was uniquely produced by T<sub>H2</sub> clones: Whereas T<sub>H2</sub> and “T<sub>H9</sub>” clones expressed little IL-9 in the resting state, up-regulation of IL-9 was observed after activation of clones generated from the CCR4<sup>+</sup>/CCR8<sup>+</sup> population (Fig. 2, A and C). Analysis of cytokine profiles in the resting state showed that IL-9-producing clones express high levels of IL-5 and IL-13 even at significantly higher levels than “conventional” CCR4<sup>+</sup>/CCR8<sup>-</sup> T<sub>H2</sub> clones (Fig. 2B). Comparison of cytokine profiles in the resting state and after activation confirmed that all T<sub>H</sub> cell clones with the ability to produce IL-9 after activation express high levels of IL-13—but not interferon-γ (IFN-γ) or IL-17—in the resting state (Fig. 2, D and E, and fig. S1C). On the basis of these findings, we termed the subpopulation of T<sub>H2</sub> cells with the ability to express IL-9 after activation as “IL-9<sup>+</sup> T<sub>H2</sub> cells.”

### The “T<sub>H9</sub>” phenotype results from transient down-regulation of signature T<sub>H2</sub> cytokines in IL-9<sup>+</sup> T<sub>H2</sub> cells

We next investigated the circumstances under which IL-9<sup>+</sup> T<sub>H2</sub> cells adopt the “T<sub>H9</sub>” phenotype. Previous reports showed that TCR signaling positively regulates IL-9 expression (9, 18). Therefore, we hypothesized that the “T<sub>H9</sub>” phenotype was a consequence of TCR and co-receptor activation and analyzed the cytokine profile of freshly isolated T<sub>H</sub> cells and of IL-9<sup>+</sup> T<sub>H2</sub> clones after differential activation

of the TCR complex (Fig. 3). The strength of activation correlated positively with up-regulation of IL-9, whereas cell viability was unaffected (Fig. 3, A to D, and fig. S2, A and B). In IL-9<sup>+</sup> T<sub>H2</sub> clones, up-regulation of IL-9 was paralleled by transient down-regulation of IL-4, IL-13, and, to a lesser extent, IL-5 (Fig. 3, E to H). As a result, a proportion of activated IL-9<sup>+</sup> T<sub>H2</sub> cells shows a “T<sub>H9</sub>” phenotype after activation (Fig. 3, E and G). At later time points, expression of T<sub>H2</sub> cytokines recovered, whereas IL-9 expression waned (Fig. 3, E to G).

To address a potential autocrine mechanism regulating the transient changes in cytokine profiles after activation, we neutralized or blocked IL-9, IL-9R, or IL-13 and assessed the effect on viability, cytokine production, or proliferation in IL-9<sup>+</sup> T<sub>H2</sub> clones but observed no effect (fig. S2, C to G). These findings suggest that transient changes in cytokine profiles after activation are not regulated in an autocrine manner by IL-9 or IL-13.

### IL-4 and TGF-β prime T<sub>H2</sub> cells to express IL-9

Previous studies on “T<sub>H9</sub>” cells have mainly relied on naïve T<sub>H</sub> cells that were “T<sub>H9</sub>”-primed in vitro with IL-4 and transforming growth factor-β (TGF-β) (3, 4). To test the stability of the “T<sub>H9</sub>” phenotype under these conditions, we performed time course analysis of cytokine and transcription factor expression of in vitro-primed “T<sub>H9</sub>” cells (Fig. 4). At the protein level, we observed a gradual increase of IL-9, peaking at day 7, followed by an almost complete down-regulation of IL-9 at day 11 (Fig. 4, A and B). Over this period, IL-13 expression gradually increased, thus leaving behind a population of cells with a T<sub>H2</sub> cytokine profile. At the time point of peak IL-9 production (day 7), the majority of IL-9<sup>+</sup> cells did not coexpress IL-13, thus showing a “T<sub>H9</sub>” phenotype. Thereafter, IL-9<sup>+</sup> cells started to coexpress IL-13 before IL-9 expression waned almost completely (Fig. 4B). Reactivation experiments after one round of priming showed that “T<sub>H9</sub>”-primed cells went through cycles of IL-9<sup>single+</sup> to IL-9<sup>+</sup>/IL-13<sup>+</sup> to IL-13<sup>single+</sup>, both when reactivated in nonpolarizing or in “T<sub>H9</sub>”-polarizing conditions (fig. S3). However, even three rounds of “T<sub>H9</sub>” priming failed to induce a stable population of IL-9<sup>single+</sup> cells (Fig. 4C). Consistent results were obtained at the mRNA level (Fig. 4D). “T<sub>H9</sub>” polarization strongly suppressed *IL4* transcription while inducing higher levels of both *IL5* and *IL13* at day 7 as compared with T<sub>H2</sub> polarization. This cytokine profile was reminiscent of that of the CCR4<sup>+</sup>/CCR8<sup>+</sup> IL-9-producing T<sub>H</sub> cells described above. Analysis of transcription factors implicated in the transcriptional network of “T<sub>H9</sub>” cells (19) showed no discernable difference in the expression of *SPI1*, *IRF4*, *BATF*, and *GATA3* between T<sub>H2</sub>- and “T<sub>H9</sub>”-primed cells at day 7 (Fig. 4E). Accordingly, all IL-9<sup>+</sup> cells coexpressed the T<sub>H2</sub> lineage-defining transcription factor *GATA3* at the single-cell level under “T<sub>H9</sub>”-priming conditions (Fig. 4F).

We concluded that the addition of TGF-β to in vitro priming with IL-4 endows T<sub>H2</sub> cells with the ability to express IL-9 transiently after activation and induces higher levels of IL-5 than conventional T<sub>H2</sub>-priming with IL-4 alone. However, in our hands, “T<sub>H9</sub>” priming failed to imprint a stable phenotype that was fundamentally distinct from that of T<sub>H2</sub> cells. Rather, in vitro-primed “T<sub>H9</sub>” cells showed phenotypic overlap with freshly isolated CCR4<sup>+</sup>/CCR8<sup>+</sup> IL-9<sup>+</sup> memory T<sub>H2</sub> cells.

### IL-9<sup>+</sup> T<sub>H2</sub> cells express the transcription factor PPAR-γ

We next sought to characterize the transcriptional program that differentiates IL-9<sup>+</sup> T<sub>H2</sub> cells from conventional T<sub>H2</sub> cells. We first selected representative T<sub>H1</sub>, T<sub>H17</sub>, T<sub>H2</sub>, and IL-9<sup>+</sup> T<sub>H2</sub> clones (Fig. 5A)

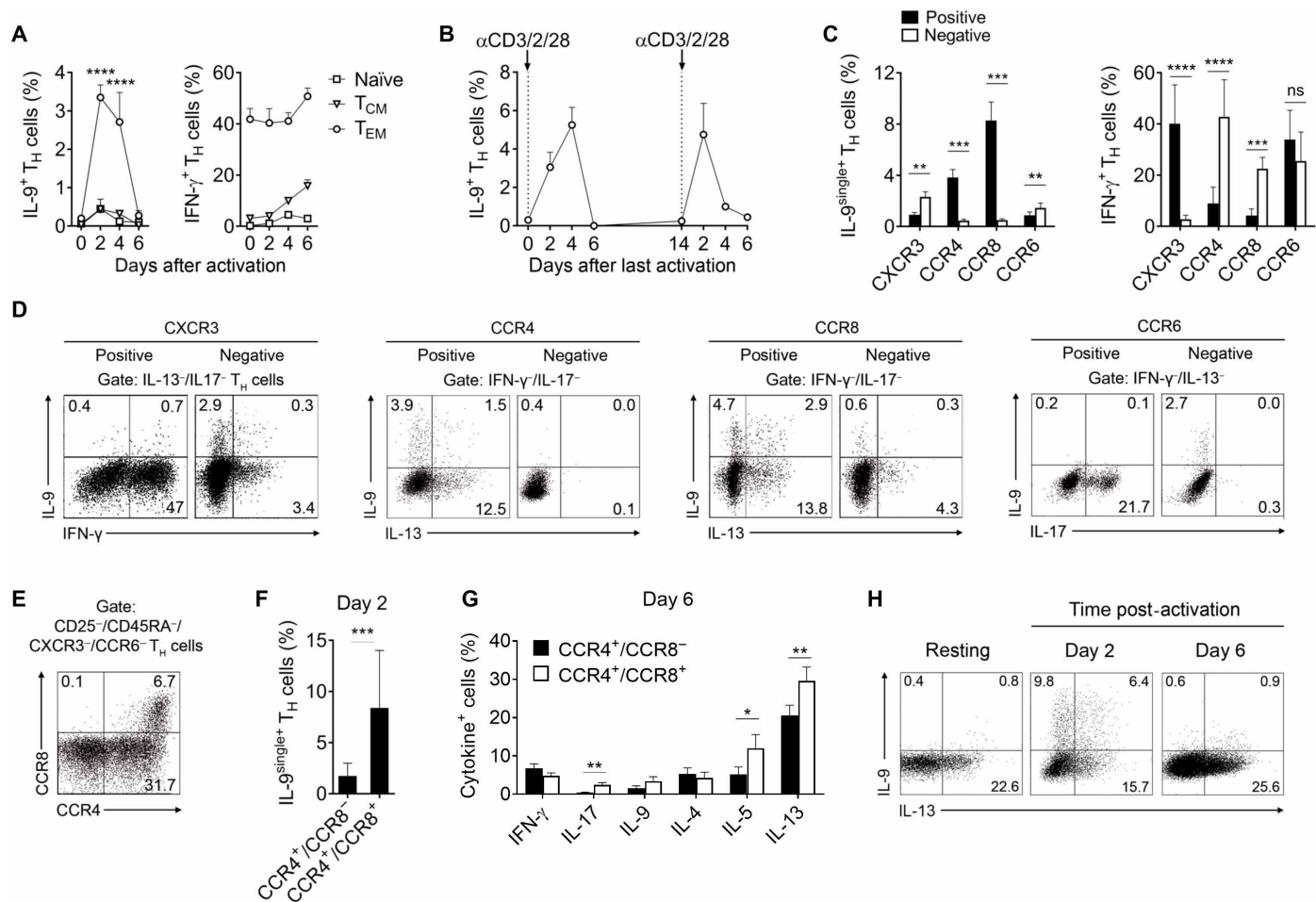


**Fig. 1. IL-9-expressing TH cells are highly enriched in CCR4<sup>+</sup>/CCR8<sup>+</sup> effector memory TH cells.** (A) Naive, central memory (T<sub>CM</sub>), and effector memory (T<sub>EM</sub>) T<sub>H</sub> cells were sorted from PBMCs of healthy donors according to the expression of CCR7, CD45RA, and CD25 and activated with  $\alpha$ CD3/CD2/CD28 beads. The production of IL-9 and IFN- $\gamma$  was assessed by flow cytometry at the indicated time points. (B) Effector memory T<sub>H</sub> cells were repeatedly activated with  $\alpha$ CD3/2/28 beads, and IL-9 production was measured at the indicated time points by flow cytometry. (C) CD4<sup>+</sup>/CD25<sup>-</sup> T cells were sorted according to the expression of the indicated chemokine receptors into positive (black bars) and negative (white bars) populations and activated with  $\alpha$ CD3/CD2/CD28 beads. On day 2, production of IFN- $\gamma$ , IL-13, IL-17, and IL-9 was simultaneously analyzed by flow cytometry (IL-9<sup>single+</sup> = IL-9<sup>+</sup>/IFN- $\gamma$ <sup>-</sup>/IL-13<sup>-</sup>/IL-17<sup>-</sup> T<sub>H</sub> cells). ns, not significant. (D) Representative plots of CXCR3-, CCR4-, CCR8-, and CCR6-positive and negative memory T cells, stimulated as in (C). (E) CCR4 and CCR8 expression in freshly isolated CXCR3<sup>-</sup>/CCR6<sup>-</sup>/CD25<sup>-</sup> memory T<sub>H</sub> cells. (F to H) CCR4<sup>+</sup>/CCR8<sup>-</sup> and CCR4<sup>+</sup>/CCR8<sup>+</sup> CD25<sup>-</sup> memory T<sub>H</sub> cells were sorted from healthy donors and activated with  $\alpha$ CD3/CD2/CD28 beads. Production of cytokines was assessed on day 2 (F) or day 6 (G) as in (C). (H) Representative example of cytokine expression in CCR4<sup>+</sup>/CCR8<sup>+</sup> CD25<sup>-</sup> memory T<sub>H</sub> cells before and at different time points after activation. Data are representative of independent experiments with at least four donors (B, G, and H) or at least six donors (A and C to F) and presented as means  $\pm$  SD. \**P* < 0.05, \*\**P* < 0.01, \*\*\**P* < 0.001, \*\*\*\**P* < 0.0001. Statistics: One-way ANOVA, followed by Tukey multiple comparison test (A), or paired two-tailed *t* test (C, F, and G).

and determined their transcriptome in the resting state. Principal components analysis and comparison of transcription factor expression confirmed that IL-9<sup>+</sup> T<sub>H</sub> cells are fundamentally related to T<sub>H</sub>2 cells (Fig. 5, B and C). To discover genes that identify resting T<sub>H</sub>2 cells with the ability to up-regulate IL-9 after activation, we determined the transcriptome of T<sub>H</sub>1, T<sub>H</sub>2, and IL-9<sup>+</sup> T<sub>H</sub>2 clones in the resting state (0 hours) and after activation (2, 4, 6, and 12 hours). We then correlated gene expression in the resting state with expression of *IL9* after activation and ranked the genes according to the mean correlation index (Fig. 5D and fig. S4). We found a strong correlation between a T cell's expression level of *PPARG* in the resting state (0 hours) and its ability to up-regulate *IL9* after activation (2, 4, 6, and 12 hours; *R*<sub>mean</sub> = 0.957) (Fig. 5E). Accordingly, *PPARG* expression was significantly enriched in resting IL-9<sup>+</sup> T<sub>H</sub>2 clones

(Fig. 5F). In addition, *PPARG* expression was found to be strongly and rapidly induced after activation (peak 4 hours after activation) and thus to precede the up-regulation of *IL9* (Fig. 5G). These findings were substantiated in freshly isolated memory T<sub>H</sub> cells. In the resting state, CCR8<sup>+</sup> T<sub>H</sub>2 cells express higher levels of *PPARG* than CCR8<sup>-</sup> T<sub>H</sub>2 cells, whereas T<sub>H</sub>1 cells lack relevant *PPARG* expression (Fig. 5H). Furthermore, activation leads to strong induction of *PPARG* almost exclusively in CCR8<sup>+</sup> T<sub>H</sub>2 cells (Fig. 5H). Together, these data uncovered an association of *PPARG* and activation-induced IL-9 expression in CCR8<sup>+</sup> memory T<sub>H</sub> cells.

To verify whether *PPARG* is also induced by “T<sub>H</sub>9” priming in vitro, we determined *PPARG* levels at days 3 and 7 in T<sub>H</sub>0-, T<sub>H</sub>2-, and “T<sub>H</sub>9”-primed cells (Fig. 5I). As recently described (20, 21), *PPARG* was induced by T<sub>H</sub>2 priming. However, “T<sub>H</sub>9” priming induced significantly

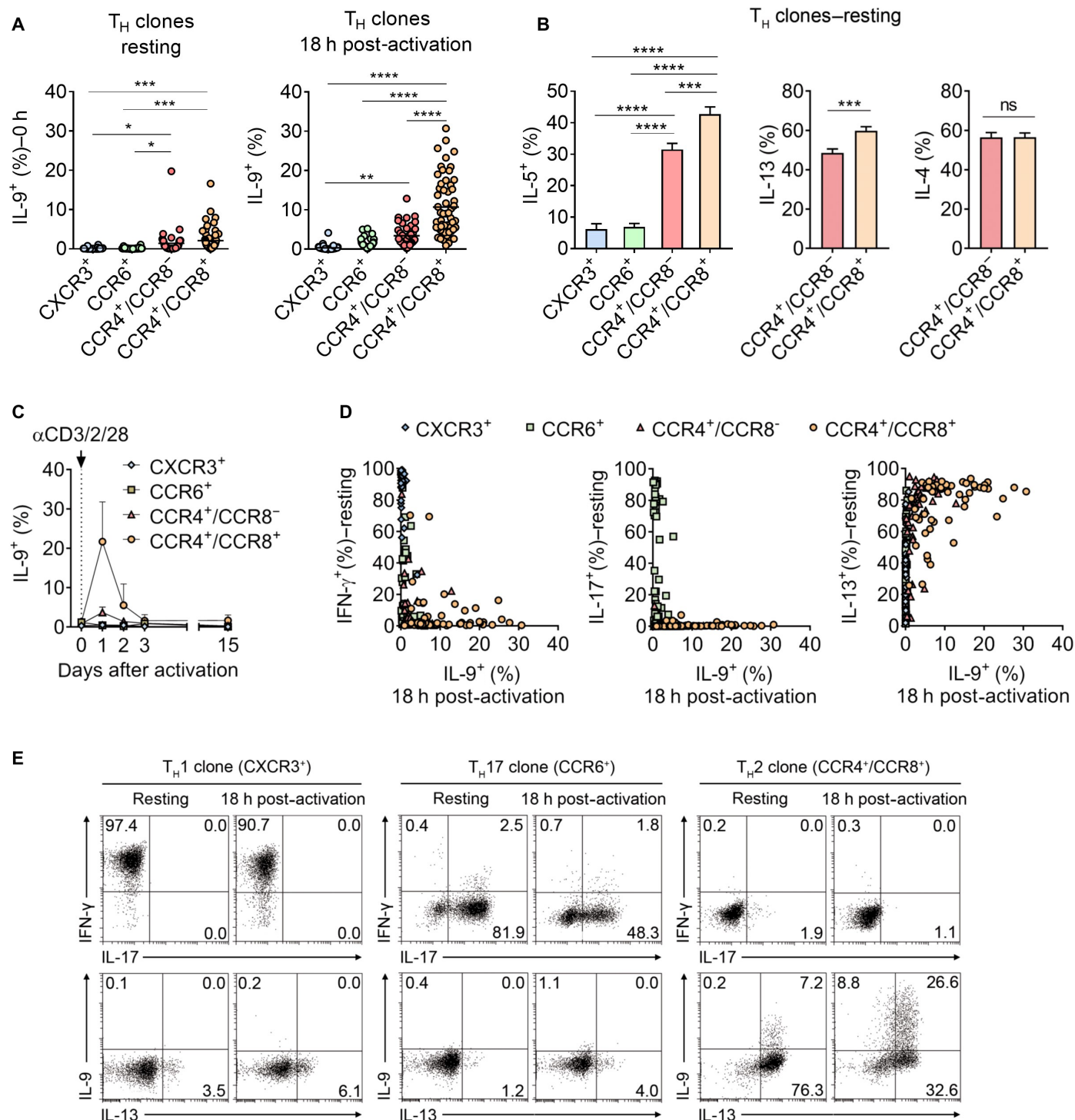


**Fig. 2. IL-9-expressing TH cell clones express high levels of TH2 cytokines in the resting state.** Single cells from memory TH cell subsets were isolated from healthy donors according to the expression of chemokine receptors and used to generate TH cell clones: CXCR3<sup>+</sup>/CCR4<sup>-</sup>/CCR6<sup>-</sup> (“CXCR3<sup>+</sup>,” enriched for TH1), CXCR3<sup>-</sup>/CCR4<sup>+</sup>/CCR6<sup>+</sup> (“CCR6<sup>+</sup>,” enriched for TH17), CXCR3<sup>-</sup>/CCR4<sup>+</sup>/CCR6<sup>-</sup> (“CCR4<sup>+</sup>,” enriched for TH2), and CXCR3<sup>-</sup>/CCR4<sup>+</sup>/CCR6<sup>+</sup>/CCR8<sup>+</sup> (“CCR4<sup>+</sup>/CCR8<sup>+</sup>,” enriched for “TH9”). (A) TH cell clones were analyzed in the resting state (left graph) and at 18 hours after activation with αCD3/CD2/CD28 beads (right graph) for their expression of IL-9. (B) TH cell clones were analyzed in the resting state for their expression of IL-4, IL-5, and IL-13. (C) Time course analysis of IL-9 expression in TH cell subset clones after activation with αCD3/CD2/CD28 beads as measured by flow cytometry. (D) Cytokine production of unselected TH cell subset clones in the resting state (y axis) compared with IL-9 production 18 hours after activation (x axis) as measured by flow cytometry. Each dot represents a single TH cell clone. (E) Representative examples of cytokine profiles of TH cell subset clones in the resting state and at 18 hours after activation. Data are representative of independent experiments with at least four (C) or six (A, B, D, and E) donors and presented as means ± SD. \*P < 0.05, \*\*P < 0.01, \*\*\*P < 0.001, \*\*\*\*P < 0.0001. Statistics: One-way ANOVA, followed by Tukey multiple comparison test (A and B, left), or unpaired t test (B, middle and right).

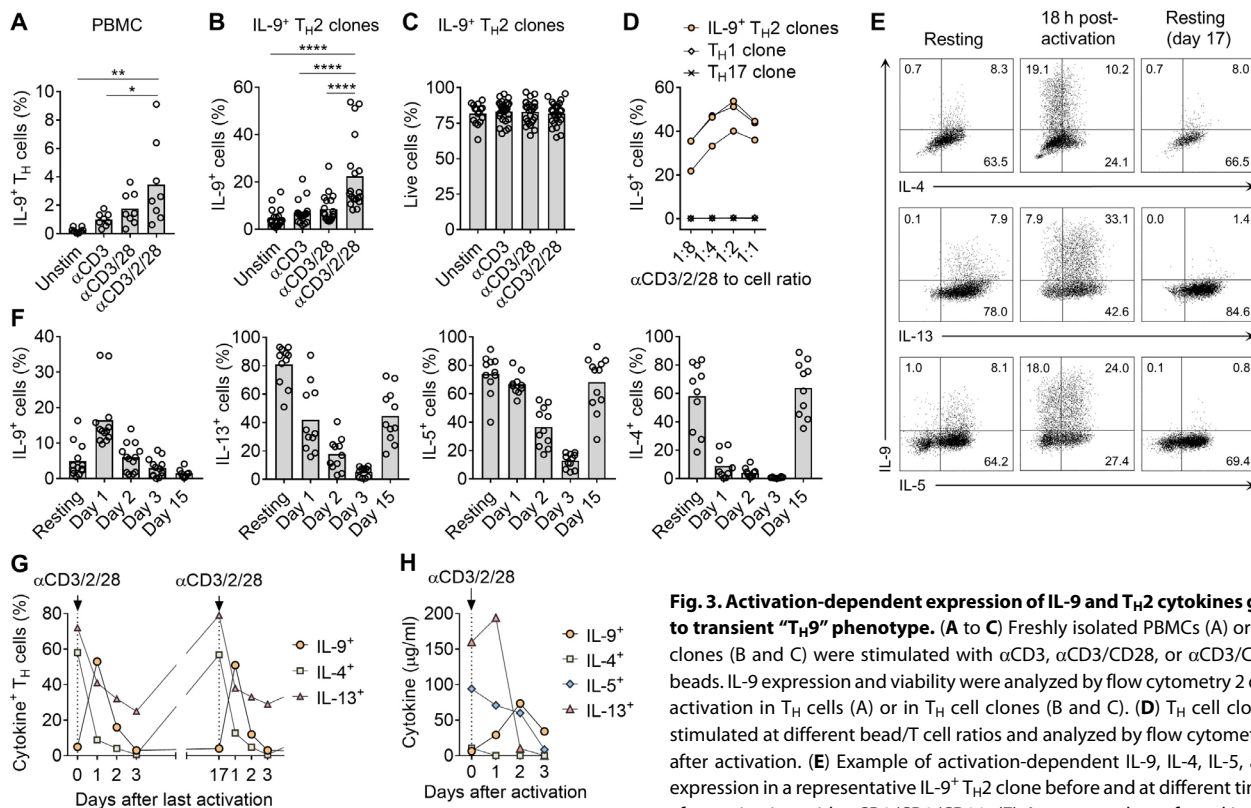


**Fig. 3. Activation-dependent expression of IL-9 and T<sub>H2</sub> cytokines gives rise to transient “T<sub>H9</sub>” phenotype.** (A to C) Freshly isolated PBMCs (A) or IL-9<sup>+</sup> T<sub>H2</sub> clones (B and C) were stimulated with αCD3, αCD3/CD28, or αCD3/CD2/CD28 beads. IL-9 expression and viability were analyzed by flow cytometry 2 days after activation in T<sub>H</sub> cells (A) or in T<sub>H</sub> cell clones (B and C). (D) T<sub>H</sub> cell clones were stimulated at different bead/T cell ratios and analyzed by flow cytometry 2 days after activation. (E) Example of activation-dependent IL-9, IL-4, IL-5, and IL-13 expression in a representative IL-9<sup>+</sup> T<sub>H2</sub> clone before and at different time points after activation with αCD3/CD2/CD28. (F) Aggregate data of cytokine production

by IL-9<sup>+</sup> T<sub>H2</sub> clones before and at different time points after activation with αCD3/CD2/CD28 beads. Analysis as in (B). (G and H) IL-9 and T<sub>H2</sub> cytokine expression kinetics after repeated activation of a representative IL-9<sup>+</sup> T<sub>H2</sub> clone, as analyzed at the indicated time points by flow cytometry (G) or in cell culture supernatants (H). Data are representative of independent experiments with clones from four donors (A to F) or one representative clone (G and H) and presented as means ± SD. \**P* < 0.05, \*\**P* < 0.01, \*\*\*\**P* < 0.0001. Statistics: One-way ANOVA, followed by Tukey multiple comparison test.

higher and stable levels of *PPARG* and reactivation strongly up-regulated *PPARG* in “T<sub>H9</sub>”-primed, but not T<sub>H2</sub>- or T<sub>H0</sub>-primed, cells (Fig. 5J and fig. S5A). We concluded that the addition of TGF-β to T<sub>H2</sub> priming with IL-4 induces activation-dependent expression of both IL-9 and *PPAR-γ* in T<sub>H2</sub> cells.

Further genes that highly correlated with *IL9* in our correlation analysis included the cytokine receptors *IL7R* and *IL6R*, as well as T<sub>H2</sub>-associated genes such as the homing receptors *CCR4* and *PTGDR2* (CRTh2) and the chemokines *CCL17* and *CCL22* (Fig. 5D; *R*<sub>mean</sub> ≥ 0.758). To further investigate our dataset, we confirmed high expression of IL-7Rα at the protein level on IL-9<sup>+</sup> T<sub>H2</sub> clones (fig. S6, A and B). Activation of in vitro-primed “T<sub>H9</sub>” cells or IL-9<sup>+</sup> T<sub>H2</sub> clones in the presence of IL-7 did not increase IL-9 expression (fig. S6, C and D). Because the IL-7Rα chain forms the thymic stromal lymphopoietin receptor (TSLP-R) together with the TSLP-Rα chain (*CRLF2*) and TSLP is a tissue alarmin involved in epithelial type 2 responses, we investigated whether IL-9<sup>+</sup> T<sub>H2</sub> cells are responsive to TSLP. TSLP-Rα expression was enriched on CCR4<sup>+</sup>/CCR8<sup>+</sup> T<sub>H</sub> cells and on IL-9<sup>+</sup> T<sub>H2</sub> clones (fig. S6, E and F), and activation of IL-9<sup>+</sup> T<sub>H2</sub> cells in the presence of TSLP did enhance IL-9 expression (fig. S6G). High expression of IL-6Rα was also confirmed at the protein level on CCR4<sup>+</sup>/CCR8<sup>+</sup> T<sub>H</sub> cells (fig. S7, A and B). IL-6 increased early IL-9 production in differentiating “T<sub>H9</sub>” cells (fig. S7C). Together, these data indicate that both in vitro-primed and ex vivo-isolated IL-9<sup>+</sup> T<sub>H2</sub> cells express the transcription factor *PPAR-γ* and functional receptors for tissue alarmins.

### Blocking *PPAR-γ* inhibits expression of IL-9 in T<sub>H2</sub> cells

To address the functional importance of *PPAR-γ* in T<sub>H</sub> cells, we analyzed the effect of the *PPAR-γ* antagonist GW9662 on cytokine production of in vitro-primed T<sub>H</sub> cells, T<sub>H</sub> cell clones, and CCR4<sup>+</sup>/CCR8<sup>+</sup> memory T<sub>H</sub> cells, respectively (Fig. 6 and fig. S8) (20). Cytokine profiles were determined in both resting and activated T<sub>H</sub> cells after 48-hour preincubation with the antagonist (Fig. 6, A to C). IL-9 was consistently down-regulated in a dose-dependent manner by *PPAR-γ* antagonism in all T<sub>H</sub> cell populations tested. IL-5 and IL-13 expression was not affected by GW9662 in primed T<sub>H2</sub> cells and in T<sub>H2</sub> clones, whereas weak inhibition of IL-4 was observed in in vitro-primed T<sub>H2</sub> cells (Fig. 6A). *PPARG* gene silencing in IL-9<sup>+</sup> T<sub>H2</sub> clones and CCR4<sup>+</sup>/CCR8<sup>+</sup> memory T<sub>H</sub> cells by endoribonuclease prepared mixtures of small interfering RNA (siRNA) confirmed the results obtained with GW9662 (Fig. 6, D and E, and fig. S8, G and H). Production of IFN-γ in T<sub>H1</sub> cells or IL-17 in T<sub>H17</sub> clones was unaffected by *PPAR-γ* antagonism (Fig. 6, A and B, and fig. S8, A and C). Viability of T<sub>H</sub> cells was not affected by GW9662 (fig. S8B).

To investigate the differential effects of GW9662 on T<sub>H2</sub> cytokine production in T<sub>H</sub> cell clones, in vitro-primed cells, and ex vivo-activated T<sub>H</sub> cells, we compared the relative levels of *PPARG* in these cell types and analyzed cytokine-specific dose responses to GW9662. T<sub>H</sub> cell clones expressed higher levels of *PPARG* than in vitro-primed or ex vivo-isolated T<sub>H</sub> cells (fig. S8E), whereas T<sub>H2</sub> cytokines IL-4, IL-5, and IL-13 were inhibited at higher concentrations of GW9662 (fig. S8G). As a consequence, inhibitory effects of

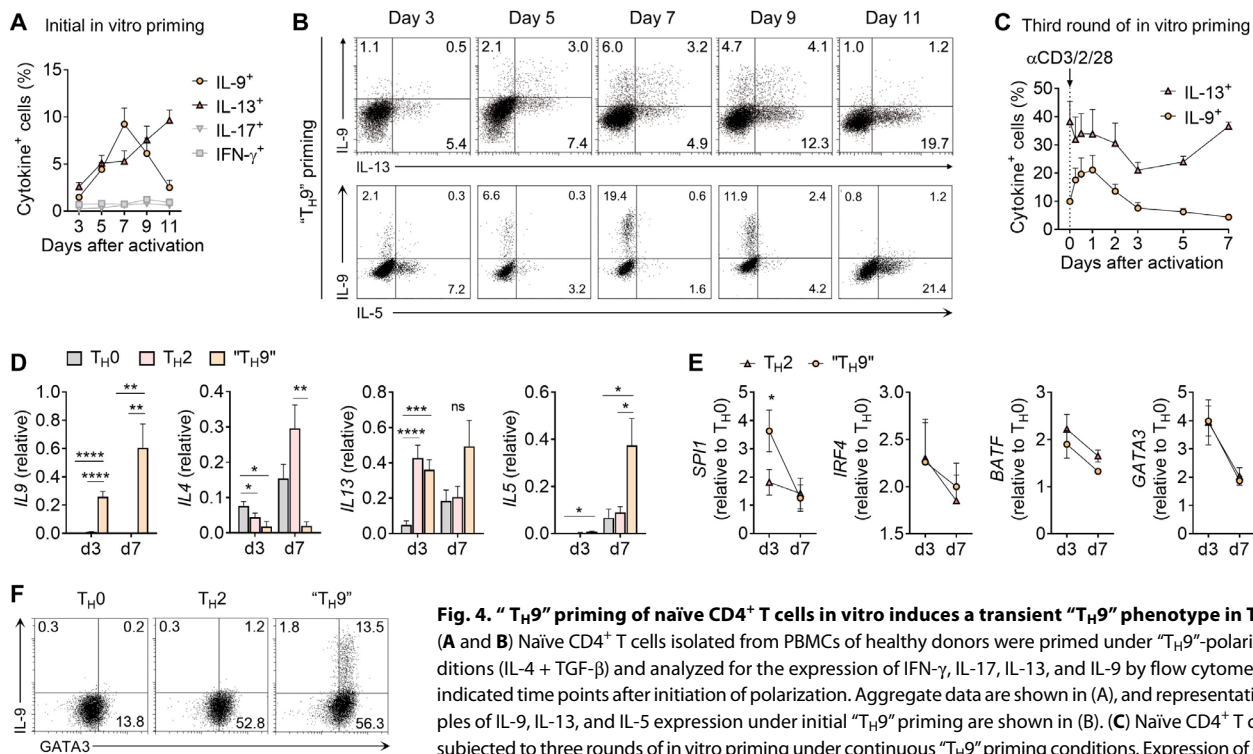


**Fig. 4. “T<sub>H</sub>9” priming of naïve CD4<sup>+</sup> T cells in vitro induces a transient “T<sub>H</sub>9” phenotype in T<sub>H</sub>2 cells.**

(A and B) Naïve CD4<sup>+</sup> T cells isolated from PBMCs of healthy donors were primed under “T<sub>H</sub>9”-polarizing conditions (IL-4 + TGF- $\beta$ ) and analyzed for the expression of IFN- $\gamma$ , IL-17, IL-13, and IL-9 by flow cytometry at the indicated time points after initiation of polarization. Aggregate data are shown in (A), and representative examples of IL-9, IL-13, and IL-5 expression under initial “T<sub>H</sub>9” priming are shown in (B). (C) Naïve CD4<sup>+</sup> T cells were subjected to three rounds of in vitro priming under continuous “T<sub>H</sub>9” priming conditions. Expression of cytokines was measured during the third round of priming at the indicated time points by flow cytometry. (D to F) Naïve

CD4<sup>+</sup> T cells were primed under T<sub>H</sub>0, T<sub>H</sub>2 (IL-4), or “T<sub>H</sub>9” (IL-4 + TGF- $\beta$ ) priming conditions, and expression of cytokines (D) or transcription factors (E and F) was measured by RT-PCR on days 3 and 7 (D and E) or by flow cytometry on day 7 (F). Data are representative of independent experiments with two (C), three (F), or at least five (A, B, D, and E) donors and presented as means  $\pm$  SD. \* $P$  < 0.05, \*\* $P$  < 0.01, \*\*\* $P$  < 0.001, \*\*\*\* $P$  < 0.0001. Statistics: One-way ANOVA, followed by Tukey multiple comparison test (D), or paired two-tailed  $t$  test (E).

GW9662 are dose and cell type dependent and affect individual cytokines differentially. Overall, however, antagonism of PPAR- $\gamma$  preferentially down-regulated IL-9 in T<sub>H</sub>2 cells.

To determine whether PPAR- $\gamma$  agonists conversely promote IL-9 production, we tested endogenous ligands [prostaglandin D2 (PGD2) and 15-deoxy- $\Delta$ -12,14-prostaglandin J2 (15d-PGJ2)] and synthetic agonists (pioglitazone and troglitazone) for their ability to induce IL-9. We did not observe any induction of IL-9 or other T<sub>H</sub>2 cytokines in IL-9<sup>+</sup> T<sub>H</sub>2 clones or in vitro-primed “T<sub>H</sub>9” cells (fig. S9). These findings are in line with those from murine T<sub>H</sub>2 cells, where PPAR- $\gamma$  agonism did not promote T<sub>H</sub>2 cytokine production (21).

### IL-9<sup>+</sup> T<sub>H</sub>2 cells expressing PPAR- $\gamma$ are present in acute allergic skin disease

On the basis of previous observations suggesting the presence of “T<sub>H</sub>9” cells in inflammatory skin disease, we sought to validate our findings in primary T<sub>H</sub> cells isolated from skin of patients with T cell-driven skin disease. Because T<sub>H</sub> cells from blood only express IL-9 after TCR activation, we hypothesized that IL-9 is up-regulated in acute, antigen-driven inflammatory skin disease. To test this, we measured *IL9* expression in normal skin (NS), chronic plaque psoriasis (cPS), and chronic atopic dermatitis (cAD) and compared it with acute guttate psoriasis (aPS), house dust mite-induced atopy test reactions (aAD), and acute contact dermatitis reactions to nickel (aACD) (Fig. 7A). *IL9* was consistently up-regulated in acute skin inflammation when compared with chronic disease and showed the highest induction in aACD. In both cAD and aACD, levels of *IL9* in the skin correlated positively with severity of disease (Fig. 7B).

In aACD, skin T cells are activated through the TCR by allergen, after which they mediate acute skin inflammation (22). Because *IL9* induction was highest in aACD, and aACD can be elicited in a controlled manner by skin patch testing, we used this model to study *IL9* production in T<sub>H</sub> cells that were activated in vivo: *IL9* was up-regulated 48 hours after elicitation of aACD and almost completely down-regulated by 120 hours, whereas *IFNG* was expressed in a more stable fashion, suggesting that IL-9 is transiently expressed by in vivo-activated T cells (Fig. 7C).

We next investigated whether IL-9-producing T<sub>H</sub> cells in skin disease are a subpopulation of T<sub>H</sub>2 cells by characterizing the cytokine profiles of T<sub>H</sub> cells isolated from inflammatory skin disease. We found the highest numbers of IL-9<sup>+</sup> T<sub>H</sub> cells in aACD when compared with other inflammatory skin disease (Fig. 7D). Of these IL-9<sup>+</sup> T<sub>H</sub> cells, the majority ( $\geq 82\%$ ) either was IL-9<sup>single+</sup> (lacking IFN- $\gamma$ , IL-17, and IL-13 expression) or coexpressed IL-13 alone (Fig. 7E and fig. S10, A and C). Only a minor proportion of IL-9<sup>+</sup> T<sub>H</sub> cells coexpressed IL-17 ( $\leq 23\%$ ) or IFN- $\gamma$  ( $\leq 8\%$ ). Many of these IL-9<sup>+</sup>/IFN- $\gamma$ <sup>+</sup> or IL-9<sup>+</sup>/IL-17<sup>+</sup> T<sub>H</sub> cells were polyfunctional T<sub>H</sub> cells that also expressed IL-13, IFN- $\gamma$ , or both (fig. S10B). In contrast, IL-9<sup>+</sup>/IL-13<sup>+</sup> T<sub>H</sub> cells did not express IL-17 or IFN- $\gamma$ . Thus, in agreement with our findings in circulating T<sub>H</sub> cells, most IL-9<sup>+</sup> T<sub>H</sub> cells in inflammatory skin disease show a T<sub>H</sub>2 or a “T<sub>H</sub>9” phenotype. These “T<sub>H</sub>9” cell lines were found to up-regulate T<sub>H</sub>2 cytokines at later time points after activation (Fig. 7, F and G, and fig. S10D), suggesting that IL-9<sup>single+</sup> cells from skin adopt a T<sub>H</sub>2 phenotype later after activation. To substantiate these findings, we generated T<sub>H</sub> cell lines and clones from blister fluid of aACD reactions. All T<sub>H</sub> cell lines

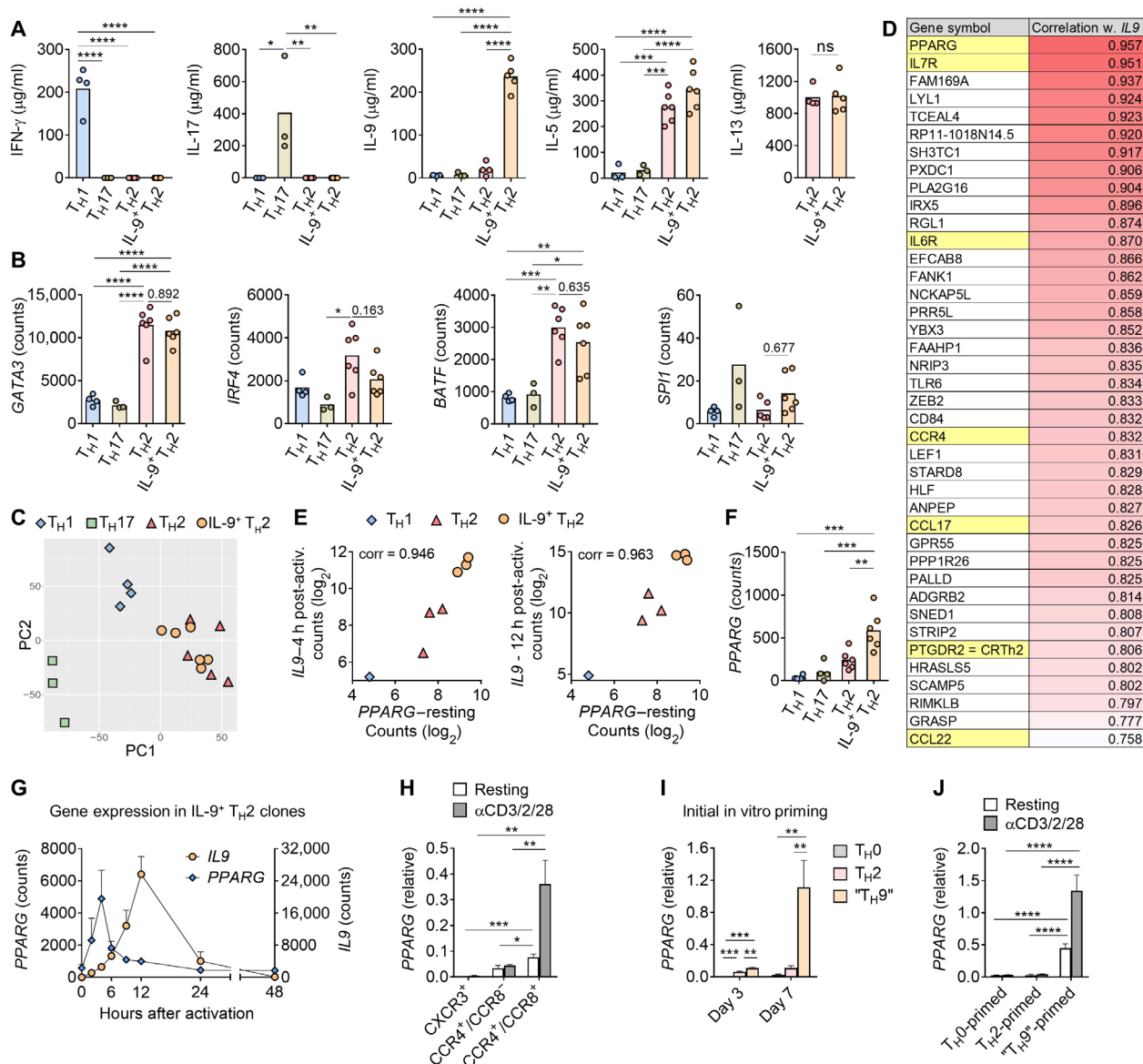


**Fig. 5. TGF- $\beta$  and IL-4 induce the expression of the transcription factor PPAR- $\gamma$  in IL-9<sup>+</sup> TH<sub>2</sub> cells.** (A to C) TH<sub>1</sub>, TH<sub>17</sub>, TH<sub>2</sub>, and IL-9<sup>+</sup> TH<sub>2</sub> clones were subjected to RNA-seq analysis in resting state. (A) Clones were selected on the basis of cytokine secretion, as measured by bead-based immunoassay 2 days after activation. (B) Transcription factor expression at resting state in TH<sub>1</sub>, TH<sub>17</sub>, TH<sub>2</sub>, and IL-9<sup>+</sup> TH<sub>2</sub> clones, as determined by RNA-seq. (C) Principal components (PC) analysis of transcriptomes of clones. (D to G) Representative TH<sub>1</sub>, TH<sub>2</sub>, and IL-9<sup>+</sup> TH<sub>2</sub> clones were subjected to RNA-seq analysis in resting state and at different time points after activation. (D) Gene expression in resting state was correlated with *IL9* expression after activation for all clones and for every gene. A ranked list of the top correlating genes (Pearson’s linear correlation coefficient) is shown. TH<sub>2</sub>-related genes are highlighted. (E) Correlation of *PPARG* expression at resting state (0 hours) and *IL9* at 4 and 12 hours after activation. (F) *PPARG* expression at resting state (0 hours) in TH<sub>1</sub>, TH<sub>17</sub>, TH<sub>2</sub>, and IL-9<sup>+</sup> TH<sub>2</sub> clones. (G) Expression time course of *PPARG* and *IL9* in IL-9<sup>+</sup> TH<sub>2</sub> clones as measured by RNA-seq. (H) *PPARG* expression was measured in ex vivo-isolated TH<sub>1</sub> (CXCR3<sup>+</sup>), TH<sub>2</sub> (CCR4<sup>+</sup>/CCR8<sup>+</sup>), and IL-9<sup>+</sup> TH<sub>2</sub> (CCR4<sup>+</sup>/CCR8<sup>+</sup>) memory TH cells in the resting state and at 4 hours after activation with  $\alpha$ CD3/CD2/CD28 by RT-PCR. (I and J) Naïve TH cells were primed under TH<sub>0</sub>-, TH<sub>2</sub>-, or “TH<sub>9</sub>”-polarizing conditions. *PPARG* expression was analyzed during (I) initial priming or (J) at day 10 (resting) and 12 hours after activation with  $\alpha$ CD3/CD2/CD28. Data are representative of independent experiments with one (A to G), six (H), or five (I and J) donors and presented as means  $\pm$  SD. \**P* < 0.05, \*\*\**P* < 0.01, \*\*\*\**P* < 0.001, \*\*\*\*\**P* < 0.0001. Statistics: One-way ANOVA, followed by pairwise comparison using Tukey multiple comparison test (A, B, F, and H to J), or Pearson’s linear correlation coefficients (D and E).

and clones that up-regulated IL-9 after activation expressed high levels of IL-13 and IL-5, but not IFN- $\gamma$  or IL-17, in the resting state (Fig. 7H and fig. S11, C and D). Together, the results obtained using aACD as in vivo model supported our previous findings by replicating that IL-9 is predominantly expressed by TH<sub>2</sub> cells in an activation-dependent and transient manner.

On the basis of the importance of PPAR- $\gamma$  in driving IL-9 expression in TH<sub>2</sub> cells from the circulation, we examined the expression of PPAR- $\gamma$  in AD and aACD (Fig. 7, I to N). *PPARG* expression was moderately up-regulated in AD and strongly up-regulated in aACD (Fig. 7I), thus reflecting the expression pattern found for IL-9 in the same skin samples (Fig. 7, A and D). Immunohistochemistry

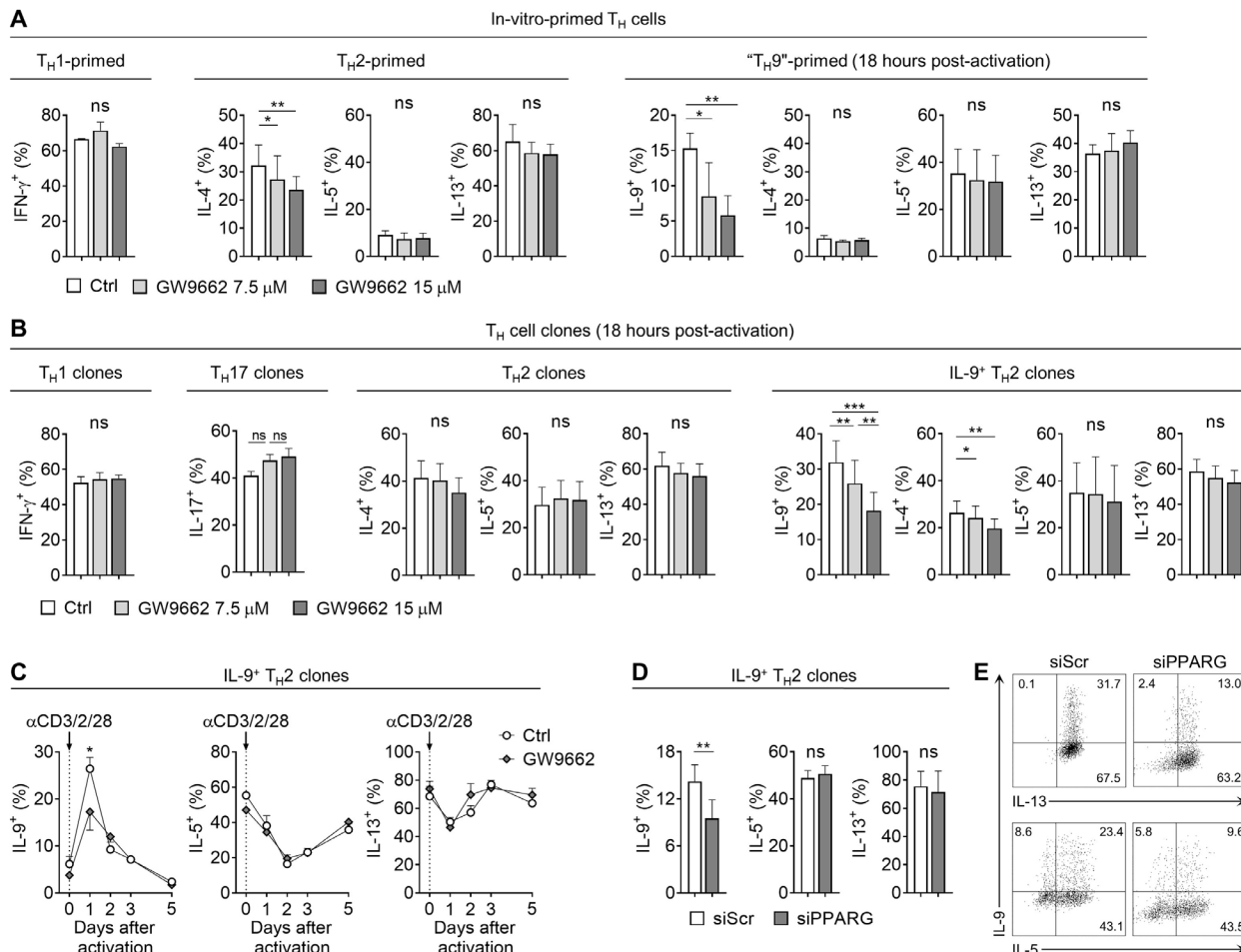


**Fig. 6. PPAR- $\gamma$  regulates IL-9 expression in  $T_H2$  cells.** (A) In vitro-primed  $T_H1$ ,  $T_H2$ , and “ $T_H9$ ” cells or (B)  $T_H1$ ,  $T_H17$ ,  $T_H2$ , and IL-9 $^+$   $T_H2$  clones were incubated for 48 hours with either the PPAR- $\gamma$  antagonist GW9662 or solvent (DMF) as control. Cytokine production was then measured by flow cytometry in resting cells or in cells activated with  $\alpha$ CD3/CD2/CD28 for 18 hours (as indicated). (C) IL-9 $^+$   $T_H2$  clones were pretreated and activated as in (B), and cytokine production was measured by flow cytometry at the indicated time points after activation. (D and E) IL-9 $^+$   $T_H2$  clones were transfected with *PPARG* or control siRNA and activated with  $\alpha$ CD3/CD2/CD28. After 1 day, cytokines were measured by flow cytometry. Aggregate data in (D) and example FACS plots in (E). Data are representative of independent experiments with at least two (A, D, and E), three (C), or five donors (B) and presented as means  $\pm$  SD. \* $P$  < 0.05, \*\* $P$  < 0.01, \*\*\* $P$  < 0.001. Statistics: One-way ANOVA, followed by Tukey multiple comparison test (A and B), or paired two-tailed *t* test (C and D).

confirmed that PPAR- $\gamma$  $^+$  cells are significantly enriched in the inflammatory infiltrate of AD and aACD (Fig. 7J and fig. S11A). Simultaneous immunofluorescence staining for PPAR- $\gamma$ , CD3, and CD4 showed that a proportion of these PPAR- $\gamma$  $^+$  cells are  $T_H$  cells (Fig. 7, K and L). *PPARG* was also highly expressed in representative IL-9 $^+$   $T_H2$  clones but not in  $T_H1$  or  $T_H17$  clones that were generated from blister fluid cells of aACD (Fig. 7M). Last, we confirmed in  $T_H2$  cell lines generated from lesion skin of aACD that antagonism of PPAR- $\gamma$  with GW9662 reduces IL-9 production in a dose-dependent manner while leaving IL-5 and IL-13 expression unaffected (Fig. 7N and fig. S11B). On the basis of these findings, we propose that in acute allergic skin inflammation, IL-9 is predominantly expressed by  $T_H2$  cells in a PPAR- $\gamma$ -dependent manner.

## DISCUSSION

On the basis of a systematic characterization of human IL-9-expressing  $T_H$  cells, we propose that “ $T_H9$ ” cells are a transient activation-

induced subpopulation of  $T_H2$  cells rather than a bona fide  $T_H$  cell lineage. Most IL-9 $^+$   $T_H$  cells are CCR4 $^+$ /CCR8 $^+$ ; express canonical  $T_H2$  cytokines, transcription factors, and chemokine receptors in the resting state; and infiltrate the skin during acute skin inflammation. In these IL-9 $^+$   $T_H2$  cells, IL-9 production is positively regulated by the transcription factor PPAR- $\gamma$ , which, in turn, is induced in naïve T cells by priming with IL-4 and TGF- $\beta$ , just as IL-9 itself.

Whether IL-9-producing  $T_H$  cells constitute an epigenetically and functionally distinct subset of  $T_H$  cells is a contentious issue. This is likely related to their transient nature and the lack of a clear physiological context in which they have been documented. Many characteristics of “ $T_H9$ ” cells could also be reconciled with their identity as a subpopulation of IL-9-expressing  $T_H2$  cells: First, “ $T_H9$ ” cells have been proposed as a distinct subset because they produce IL-9 in the absence of expression of other lineage-defining cytokines (4). Our results suggest that this is the result of partly reciprocal expression kinetics of IL-9 and signature  $T_H2$ -cytokines after activation. Second, characterization of “ $T_H9$ ” cells has strongly depended

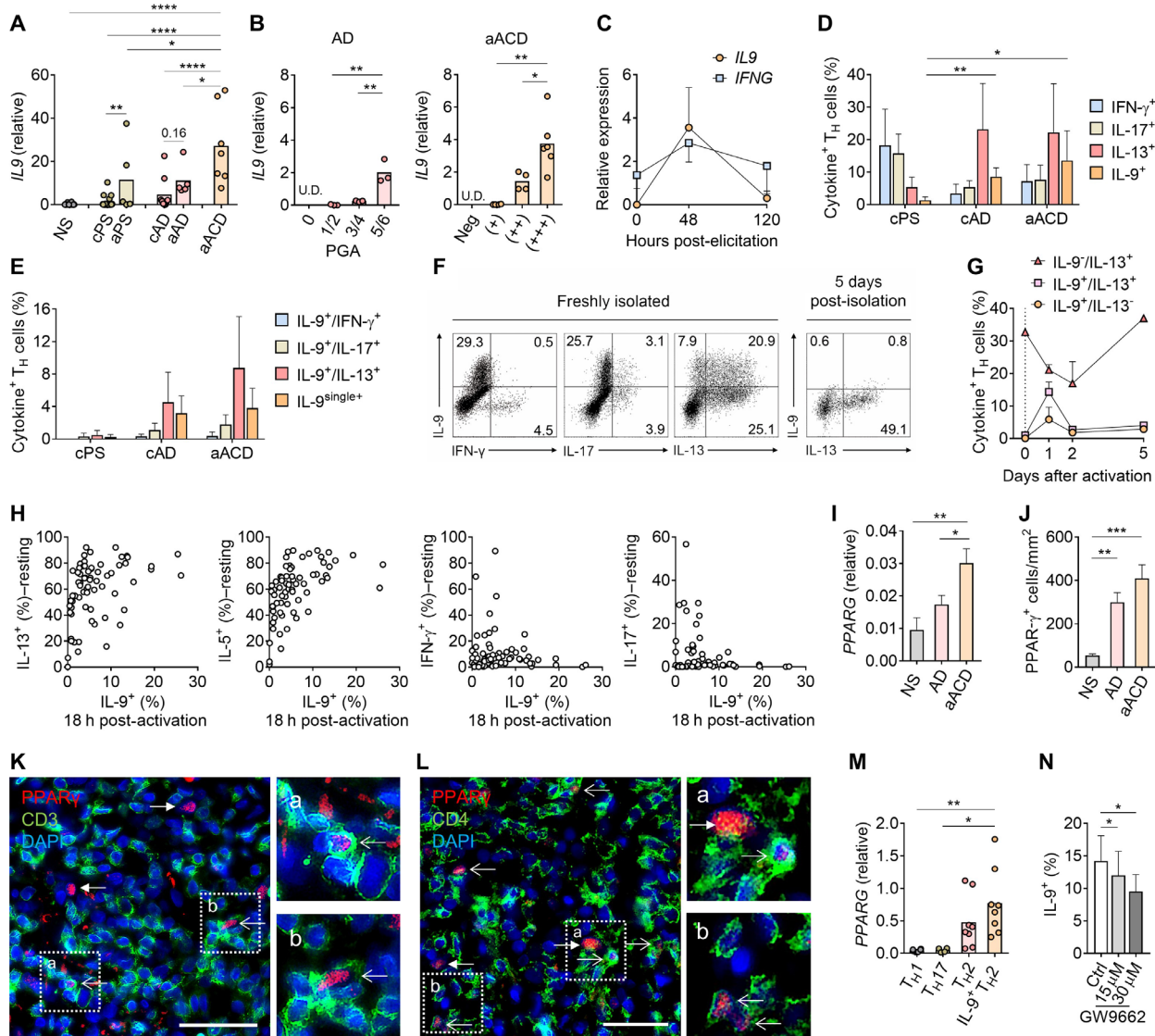


**Fig. 7. IL-9-expressing PPAR- $\gamma$ <sup>+</sup> T<sub>H</sub>2 cells infiltrate acute allergic skin inflammation.** (A) *IL9* expression was analyzed by RT-PCR in NS and in lesional skin of acute or chronic psoriasis (aPS and cPS), acute or chronic atopic dermatitis (aAD and cAD), and acute allergic contact dermatitis (aACD). (B) *IL9* levels were determined in lesional skin of AD and aACD by RT-PCR and correlated with severity of disease. PGA, physician global assessment. (C) *IL9* levels in aACD skin before and at indicated time points after elicitation. (D and E) T cells were isolated from lesional skin of cPS, cAD, and aACD. T<sub>H</sub> cell expression of IL-9, IFN- $\gamma$ , IL-17, and IL-13 was simultaneously determined by flow cytometry. (F) T<sub>H</sub> cells were isolated from aACD, and cytokine profiles were determined as in (D) either directly or 5 days after in vitro culture. (G) IL-9<sup>+</sup> T<sub>H</sub>2 cell lines were generated from aACD by short-term ex vivo culture, reactivated with  $\alpha$ CD3/CD2/CD28, and subjected to time course analysis of cytokine profiles by flow cytometry. (H) T<sub>H</sub> cell clones were generated from aACD, and cytokine profiles were analyzed in the resting state or at 18 hours after activation by flow cytometry. Each dot represents a T<sub>H</sub> cell clone. (I) *PPARG* expression in NS and in lesional skin of AD and aACD. (J) Skin sections from NS, AD, and aACD were immunohistochemically stained for PPAR- $\gamma$ , and infiltrating PPAR- $\gamma$ <sup>+</sup> cells were quantified by digital image analysis. (K and L) Representative pictures of immunofluorescence for PPAR- $\gamma$  and CD3 (K) or CD4 (L) in lesional skin of aACD. Scale bars, 50  $\mu$ m. Open arrows, PPAR- $\gamma$ <sup>+</sup>/CD3<sup>+</sup> cells (K) or PPAR- $\gamma$ <sup>+</sup>/CD4<sup>+</sup> cells (L). Closed arrows, PPAR- $\gamma$ <sup>+</sup>/CD3<sup>-</sup> cells (K) or PPAR- $\gamma$ <sup>+</sup>/CD4<sup>-</sup> cells (L). DAPI, 4',6-diamidino-2-phenylindole. (M) *PPARG* expression in representative T<sub>H</sub> cell clones generated as in (H). (N) IL-9<sup>+</sup> T<sub>H</sub>2 cell lines generated from aACD were incubated for 48 hours with the PPAR- $\gamma$  antagonist GW9662 or solvent (DMF) as control. Cells were then activated with  $\alpha$ CD3/CD2/CD28 for 18 hours, and cytokine production was measured by flow cytometry. Data are representative of independent experiments with at least two (H and M), three (B, F, and G), four (C to E, K, and L), five (A), or seven (I, J, and N) donors and presented as means  $\pm$  SD. \**P* < 0.05, \*\**P* < 0.01, \*\*\**P* < 0.001, \*\*\*\**P* < 0.0001. Statistics: One-way ANOVA, followed by Tukey multiple comparison test.

on cells primed in vitro. We found that “T<sub>H</sub>9” priming with IL-4 and TGF- $\beta$  induces transient IL-9 production in T<sub>H</sub>2 cells eventually expressing high levels of IL-5, IL-13, and GATA3. These in vitro-primed cells bear close resemblance to IL-9<sup>+</sup> T<sub>H</sub>2 cells isolated from CCR4<sup>+</sup>/CCR8<sup>+</sup> memory T<sub>H</sub> cells. Third, the proposed transcriptional network of “T<sub>H</sub>9” cells shows major overlap with that of T<sub>H</sub>2

cells (19). T<sub>H</sub> cells lacking previously proclaimed “T<sub>H</sub>9”-specific transcription factors such as BATF or IRF4 not only fail to produce IL-9 but also show defective T<sub>H</sub>2 differentiation and T<sub>H</sub>2 effector functions (23, 24). Conversely, T cells lacking classical T<sub>H</sub>2 transcription factors such as GATA3 and STAT6 (signal transducer and activator of transcription 6) fail to adopt the “T<sub>H</sub>9” phenotype and lack

pathogenicity in IL-9–dependent disease models (19, 25–27). In accordance with these findings, we observed that IL-9–producing cells under “T<sub>H</sub>9” priming conditions express GATA3 and produce T<sub>H</sub>2 cytokines later after activation. Fourth, there is a significant overlap in the reported functions of T<sub>H</sub>2 and “T<sub>H</sub>9” cells, including mediation of parasite immunity, allergic inflammation (16, 28, 29), and ulcerative colitis (30). Last, evidence for the identity of IL-9–expressing T<sub>H</sub> cells as T<sub>H</sub>2 cells further includes the location of the human *IL9* gene within the cluster of T<sub>H</sub>2 cytokines on chromosome 5, the promotion of “T<sub>H</sub>9” cells by the type 2 alarmins TSLP (31) and IL-25 (32), and the almost identical activation-dependent and transient IL-9 expression in type 2 innate lymphoid cells (ILC2), the putative evolutionary precursors of T<sub>H</sub>2 cells (33, 34). Together, our suggestion that IL-9–expressing T<sub>H</sub> cells represent a subpopulation of T<sub>H</sub>2 cells is in agreement with the current literature. It is thus intriguing that single-cell fate mapping in conjunction with T<sub>H</sub>2 cytokine analysis has so far not been reported for murine T<sub>H</sub> cells despite the availability of IL-9 reporter mice (27, 34). For example, IL-9–fluorescent reporter mice have shown an essential role for IL-9 in immunity against parasitic worm infection (10). In these mice, expression of IL-9 is transient after infection and precedes the up-regulation of IL-4, IL-5, and IL-13, thereby resembling the cytokine expression kinetics of IL-9<sup>+</sup> T<sub>H</sub>2 cells described here. How our findings from human IL-9<sup>+</sup> T<sub>H</sub>2 cells compare with those from these animal models, particularly in the setting of acute allergic skin inflammation, will have to be addressed in future studies.

The idea that IL-9<sup>+</sup> T<sub>H</sub> cells are potentially a subpopulation of T<sub>H</sub>2 cells raises the question to what extent these cells differ from T<sub>H</sub>2 cells, which lack the ability to produce IL-9. Our comparative analysis identified PPAR-γ to be preferentially expressed by IL-9<sup>+</sup> T<sub>H</sub>2 cells, and functional analysis revealed that PPAR-γ is a positive regulator of IL-9 expression in T<sub>H</sub> cells. PPAR-γ has recently been shown to drive T<sub>H</sub>2-mediated immunity and immunopathology in murine models (20, 21). In humans, *PPARG* has been shown to be expressed in “pathogenic” T<sub>H</sub>2 cells (termed “T<sub>H</sub>2A” cells) as compared with conventional T<sub>H</sub>2 cells (35). However, the regulation of IL-9 by PPAR-γ has not been addressed, and the factors that induce PPAR-γ expression in differentiating T<sub>H</sub> cells remains unknown. We find that TGF-β is able to induce high levels of PPAR-γ in polarizing T<sub>H</sub>2 cells and thus uncover a putative differentiation step toward pathogenic T<sub>H</sub>2 cells. PPAR-γ also mediates the persistence of skin-resident T cells (skin T<sub>RM</sub>), which depend on TGF-β for their development (16, 36). TGF-β might thus represent a central mediator of both pathogenic T<sub>H</sub>2 and T<sub>RM</sub> cells via the induction of PPAR-γ. Consistent with such a scenario, we found increased numbers of IL-9<sup>+</sup> T<sub>H</sub>2 and PPAR-γ–expressing T<sub>H</sub> cells in skin-homing CCR4<sup>+</sup>/CCR8<sup>+</sup> T<sub>H</sub>2 cells and in T<sub>H</sub>2 cells isolated from acute ACD, a prototypical T<sub>RM</sub> cell-mediated disease (22).

Our study has a number of limitations and raises intriguing questions that remain to be addressed. For example, it remains unknown whether other T<sub>H</sub> cell subsets can acquire the ability to produce IL-9 under different physiologic or pathologic environments or whether a more stable “T<sub>H</sub>9” phenotype can be adopted in an environment not reproduced in our study. It is possible that such inflammatory environments supporting “T<sub>H</sub>9” cells are present in other tissues than the skin. Furthermore, the mechanisms that regulate transient cytokine profiles after activation that give rise to the “T<sub>H</sub>9” phenotype remain to be elucidated. Previous studies in T<sub>H</sub>17 cells suggest that such changes can be regulated via transient expres-

sion changes of transcription factors and signaling molecules (37). Last, the mechanisms that link PPAR-γ to IL-9 expression in T<sub>H</sub>2 cells remain unknown. In our hands, activation of PPAR-γ by agonists did not increase IL-9 or T<sub>H</sub>2 cytokine production. Similarly, PPAR-γ activation had only a minor effect on production of classical T<sub>H</sub>2 cytokines in murine T<sub>H</sub> cells (21, 38). PPAR-γ might thus indirectly regulate IL-9 production in T<sub>H</sub>2 cells or in a ligand-independent manner, because ligand-independent functions of PPAR-γ have been observed (39–42). In view of its well-established role in regulating metabolism, one might further speculate that PPAR-γ controls cytokine production in IL-9<sup>+</sup> T<sub>H</sub>2 cells by promoting a metabolic state that supports this phenotype (21, 43).

## MATERIALS AND METHODS

All antibodies used in this study are listed in table S2. All gating strategies for flow cytometry analysis are described in fig. S12.

### Study design/experimental design

This is an experimental laboratory study performed on human tissue samples. All studies were performed in accordance with the Declaration of Helsinki. Human blood was obtained from healthy donors from the Swiss Blood Donation Center of Bern and used in compliance with the Federal Office of Public Health (authorization no. P\_149). Skin was obtained from healthy patients undergoing cosmetic surgery procedures or from patients with psoriasis, atopic dermatitis, allergic contact dermatitis, or positive patch test reactions to standard contact allergens. The study on human patient samples was approved by the Medical Ethics Committee of the Canton of Bern, Switzerland (#088/13). Written informed consent was obtained from all patients. Mechanistic studies on cells derived from blood and human tissues were performed with in vitro assays without blinding or randomization.

### Isolation and purification of human T cell subsets from peripheral blood

Peripheral blood mononuclear cells (PBMCs) were isolated by Ficoll-Paque PLUS (GE Healthcare, UK) density gradient centrifugation. Human CD4<sup>+</sup> T cells were isolated from PBMCs using the EasySep Positive Selection Kit (STEMCELL Technologies) according to the manufacturer’s instructions. Positively selected CD4<sup>+</sup> T cells were washed with phosphate-buffered saline and stained for subsequent T<sub>H</sub> cell subset sorting. Memory T<sub>H</sub> cell subsets were sorted to more than 90% purity according to their expression of chemokine receptors from CD45RA<sup>−</sup>CD25<sup>−</sup>CD8<sup>−</sup>CD3<sup>+</sup> cells: T<sub>H</sub>1 (CXCR3<sup>+</sup>CCR8<sup>−</sup>CCR6<sup>−</sup>CCR4<sup>−</sup>), T<sub>H</sub>2 (CXCR3<sup>−</sup>CCR8<sup>−</sup>CCR6<sup>−</sup>CCR4<sup>+</sup>), T<sub>H</sub>17 (CXCR3<sup>−</sup>CCR8<sup>−</sup>CCR6<sup>+</sup>CCR4<sup>+</sup>), and “T<sub>H</sub>9” (CXCR3<sup>−</sup>CCR8<sup>+</sup>CCR6<sup>−</sup>CCR4<sup>+</sup>). Naïve T cells were sorted as CD45RA<sup>+</sup>CCR7<sup>+</sup>CD25<sup>−</sup>CD8<sup>−</sup>CD3<sup>+</sup> cells, T<sub>CM</sub> cells as CD45RA<sup>−</sup>CCR7<sup>+</sup>CD25<sup>−</sup>CD8<sup>−</sup>CD3<sup>+</sup> cells, and T<sub>EM</sub> cells as CD45RA<sup>−</sup>CCR7<sup>−</sup>CD25<sup>−</sup>CD8<sup>−</sup>CD3<sup>+</sup> cells. Sorting purity of T cell subsets was typically more than 95% post-sort analysis.

### T cell culture, T cell activation, and cytokine expression kinetics

Culture medium consisted of RPMI 1640 with HEPES (Gibco) supplemented with 5% heat-inactivated human serum (Swiss Red Cross, Basel, Switzerland), 2 mM L-glutamine (Biochrom), penicillin (50 U/ml) and streptomycin (50 μg/ml) (BioConcept), and IL-2 (50 IU/ml) (Roche). T cells were cultured at a density of 0.25 × 10<sup>5</sup>

to  $1 \times 10^5$  cells per well of a 96-well plate in a total volume of 200- $\mu$ l cell culture medium. For cytokine expression kinetics, T cells were polyclonally activated using beads coated with antibodies against CD3, CD2, and CD28 [T cell/bead = 2:1; Human T Cell Activation/Expansion Kit (Miltenyi) or ImmunoCult Human CD3/CD28/CD2 T Cell Activator (STEMCELL Technologies)]. Before activation and at different time points thereafter, T cells were additionally stimulated for 4 hours with phorbol 12-myristate 13-acetate (PMA) (50 ng/ml) and ionomycin (1  $\mu$ M) in the presence of brefeldin A (10  $\mu$ g/ml) (Sigma Chemicals) and then intracellularly stained for later analysis by flow cytometry (see below). Supernatants were collected at day 2 after polyclonal activation, and cytokines were measured as described below.

### T cell cloning

Single memory T<sub>H</sub> cells from PBMCs were directly sorted into 96-well plates according to their expression of chemokine receptors (see above). For cloning of skin T cells, infiltrating cells isolated from blister fluid of positive patch tests to nickel were cultured in cell culture medium supplemented with IL-2 (50 IU/ml) for 7 to 14 days. CD4<sup>+</sup> T cells were isolated from bulk cells using the EasySep Positive Selection Kit (STEMCELL Technologies) according to the manufacturer's instructions. CD4<sup>+</sup> T cells were seeded at 0.5 cell per well with irradiated allogeneic feeder cells ( $5 \times 10^4$  per well). Thereafter, single cells were cloned by periodic activation with phytohemagglutinin (1  $\mu$ g/ml; Sigma) and irradiated allogeneic feeder cells ( $5 \times 10^4$  per well) in culture medium. Half of the T cell culture medium was replaced by fresh medium every second day starting from day 2 after reactivation. T<sub>H</sub> cell clones were analyzed in the resting state ( $\geq 17$  days after the last expansion) or at different time points after polyclonal activation as described above.

### RNA sequencing

Total RNA was isolated from T<sub>H1</sub>, T<sub>H2</sub>, T<sub>H17</sub>, and IL-9<sup>+</sup> T<sub>H2</sub> clones with the RNAREADY Kit (AmpTec) according to the manufacturer's instruction. Samples were submitted to the Next Generation Sequencing (NGS) Platform, Institute of Genetics, University of Bern. RNA integrity was analyzed using 2100 Bioanalyzer (Agilent Technologies). For all samples, RNA integrity number values were  $\geq 8$ . Total RNA was converted into a library of template molecules with TruSeq Stranded mRNA Sample Preparation Kits (Illumina) using the robotic pipette system EpMotion 5075 (Eppendorf). Single-end 100-base pair sequencing was performed with HiSeq 3000 (Illumina). RNA-sequencing (RNA-seq) reads were mapped to the human reference genome (GRCh38, build 81) using HISAT2 v. 2.0.4. We then used HTseq-count v. 0.6.1 to count the number of reads per gene, and DESeq2 v.1.4.5 to test for differential expression between groups of samples. RNA-seq data are deposited on ArrayExpress (accession no. E-MTAB-5739).

### In vitro T cell differentiation

Sorted naive T cells were stimulated with  $\alpha$ CD3/CD28/CD2 beads (T cell/bead = 2:1, Miltenyi) and primed into effector CD4<sup>+</sup> T cell subsets without additional cytokine for T<sub>H0</sub> cells, with IL-4 (50 ng/ml) (BioLegend) for T<sub>H2</sub> cells, with IL-4 (50 ng/ml) and TGF- $\beta$  (5 ng/ml) (R&D Systems) for "T<sub>H9</sub>" cells, and with TGF- $\beta$  (5 ng/ml) (R&D Systems) for "iT<sub>reg</sub>." From initiation of cell culture until time point of analysis, culture medium was resupplemented with the indicated cytokines every other day. Cells were harvested at different time points

for real-time polymerase chain reaction (PCR) analysis or for intracellular cytokine analysis by flow cytometry.

### Functional analysis of PPAR- $\gamma$ inhibition in T cells

Functional analysis of PPAR- $\gamma$  in human T cells was performed using PPAR- $\gamma$  agonists pioglitazone (Sigma) and troglitazone (Sigma), endogenous ligands PGD2 (Sigma) and 15d-PGJ2 (Sigma), and the PPAR- $\gamma$  antagonist GW9662 (Sigma). GW9662 is a selective PPAR- $\gamma$  antagonist with an EC<sub>50</sub> (median effective concentration) of 3.3 nM in a cell-free assay. T<sub>H</sub> cell clones and in vitro-primed T<sub>H</sub> cells were preincubated for 48 hours with GW9662 (7.5 and 15  $\mu$ M) or solvent [*N,N'*-dimethylformamide (DMF)] as control. Thereafter, cells were washed and polyclonally activated for intracellular cytokine staining as described above or used for RNA isolation for later reverse transcription PCR (RT-PCR) analysis. For functional analysis of PPAR- $\gamma$  in freshly isolated T<sub>H</sub> cells, T cells from PBMCs were polyclonally activated in the presence of GW9662 (15 and 30  $\mu$ M) or solvent (DMF) for 3 days before analysis of cytokine expression by flow cytometry.

For gene silencing of PPAR- $\gamma$  by siRNA, T<sub>H</sub> cells were electroporated (4D-Nucleofector, Lonza: Buffer P3, pulse E0-115) for transfection with scrambled siRNA (sense, 5'-UUCUCCGAACGUGUCACGUdTdT-3') or PPAR- $\gamma$  siRNA (sense, 5'-GUGGGAGUGGUCUCCAUAUdTdT-3', both from Eurofins Genomics) for fig. S8G or with esiRNA human PPAR- $\gamma$  (Sigma EHU097711) for Fig. 6, D and E, and fig. S8H. Thereafter, transfected cells were activated with  $\alpha$ CD3/CD28/CD2 (STEMCELL ImmunoCult T Cell Activator), after which cells were analyzed at different time points by RT-PCR or flow cytometry.

### Measurement of cytokines by flow cytometry or bead-based immunoassay

All antibodies used in this study for flow cytometry are listed in table S2. For analysis of cytokine production, cells were stimulated with PMA (50 ng/ml), ionomycin (1  $\mu$ M), and brefeldin A (10  $\mu$ g/ml). After viability staining and surface staining, cells were fixed and permeabilized with Cytofix/CytoPerm kit (BD Biosciences) according to the manufacturer's instructions. Intracellular proteins were detected by fluorescence-labeled antibodies.

Proliferation assays were performed with carboxyfluorescein diacetate succinimidyl ester (CFSE) staining. Cells were labeled with CFSE (1:5000) and incubated at 37°C for 8 min, followed by incubation for 5 min with R9.

Supernatants were analyzed by the bead-based immunoassay from LEGENDplex Human Th Cytokine Panel (13-plex, BioLegend) according to the manufacturer's instructions. Stained cells or bead-based immunoassay were acquired on FACSCanto I (BD Biosciences) or CytoFLEX (Beckman Coulter), and data were analyzed using FACSDiva software (BD Biosciences) or CytExpert software (Beckman Coulter), respectively.

### Quantitative real-time RT-PCR

Total RNA was isolated from cultured T cells or FACS (fluorescence-activated cell sorting)-sorted T cells at different time points after polyclonal activation (as described above) with the RNAREADY Kit (AmpTec) according to the manufacturer's instructions. RNA from snap-frozen skin biopsies was isolated using the RNeasy Lipid Tissue Kit (Qiagen) according to the manufacturer's instructions. Total mRNA quality was measured with the ND-1000 Spectrophotometer (Thermo Fisher Scientific) or 2100 Bioanalyzer (Agilent). Complementary DNA

was generated using Omniscript reverse transcriptase (Qiagen). Real-time PCR was performed with TaqMan probe-based assays and measured with the 7300 Real Time PCR System (Applied Biosystems). Expression of each ligand transcript was determined relatively to the reference gene transcript (HPRT-1,  $\beta$ -actin,  $\beta$ 2M) and normalized to the target gene expression by  $2^{-\Delta\Delta Ct}$ . Data are represented as arbitrary relative units. All primers used to detect the transcripts were purchased from Life Technologies Europe B.V. and are listed in table S3.

### Isolation and activation of skin-resident T cells from skin biopsies

Punch biopsy samples were obtained from healthy patients undergoing cosmetic surgery or from patients with psoriasis, atopic dermatitis, allergic contact dermatitis, or positive patch test reactions to standard contact allergens. Patch testing for the diagnosis of contact allergy was performed and graded according to the European Society of Contact Dermatitis guideline for diagnostic patch testing (44). After biopsy, subcutaneous fat was removed, and tissue was minced and transferred into a 24-well plate with culture medium supplemented with IL-2 (100 IU/ml). After 3 to 5 days of culture, cells were isolated and filtered through 70- and 35- $\mu$ m cell strainers. Cytokine production by lymphocytes was analyzed by flow cytometry (as described above).

### Immunohistochemical staining

All antibodies used for immunohistochemical stainings are listed in table S2. Immunohistochemistry for PPAR- $\gamma$  was performed using a BOND-III fully automated immunohistochemistry and in situ hybridization stainer (Leica Biosystems) according to the manufacturer's instructions. In brief, paraffin-embedded tissue sections were first dewaxed and rehydrated, followed by epitope retrieval (Epitope Retrieval Solution 2, Leica). They were then incubated with the primary antibody or an isotype-matched control antibody for 15 min, followed by a post-primary immunoglobulin G (IgG) linker and a Poly-AP IgG reagent (Bond Polymer Refine Red Detection System, Leica). Sections were then developed in Fast Red substrate chromogen (Leica). Stained slides were scanned using the panoramic Digital Slide Scanner (3DHISTECH). For quantitative analysis, three fields (0.33 mm<sup>2</sup> each field) containing infiltrating cells in the reticular dermis were selected, and the density of cells with nuclear expression of PPAR- $\gamma$  per square millimeter was quantified using a QuPath (Queen's University Belfast) digital image analysis system.

### Statistical analysis

Statistical analysis was performed by using GraphPad Prism 7.03 software. For comparison of two groups, two-tailed Student's *t* test or paired Student's *t* test was used. For comparisons of multiple groups, one-way analysis of variance (ANOVA) was used, followed by pairwise comparison of each group and correction for multiple comparison using the Tukey test. For matched samples, paired *t* test or repeated-measures ANOVA was used. Values of *P* < 0.05 were considered statistically significant.

### SUPPLEMENTARY MATERIALS

immunology.sciencemag.org/cgi/content/full/4/31/eaat5943/DC1  
 Fig. S1. Identification of human T<sub>H</sub> cell subsets by chemokine receptor expression.  
 Fig. S2. Activation-dependent expression of cytokines in T<sub>H</sub>2 clones.  
 Fig. S3. Cytokine profile after reactivation of in vitro-primed "T<sub>H</sub>9" cells.  
 Fig. S4. Correlation values of all genes with IL-9 in T<sub>H</sub>1, T<sub>H</sub>2, and IL-9<sup>+</sup> T<sub>H</sub>2 clones.  
 Fig. S5. PPAR $\gamma$  levels during first and second rounds of in vitro priming of naive T<sub>H</sub> cells.

Fig. S6. IL-7R $\alpha$  and CRLF2 form a functional TSLP-R on IL-9<sup>+</sup> T<sub>H</sub>2 cells.  
 Fig. S7. IL-6R $\alpha$  is highly expressed on IL-9<sup>+</sup> T<sub>H</sub>2 cells, and IL-6 promotes IL-9 expression in polarizing "T<sub>H</sub>9" cells.  
 Fig. S8. Effect of PPAR- $\gamma$  inhibition by GW9662 or RNA interference on cytokine production in human T<sub>H</sub> cells.  
 Fig. S9. PPAR- $\gamma$  agonists do not promote IL-9 or T<sub>H</sub>2 cytokine expression in IL-9<sup>+</sup> T<sub>H</sub>2 cells.  
 Fig. S10. Cytokine profiles of T<sub>H</sub> cells from human inflammatory skin disease.  
 Fig. S11. PPAR- $\gamma$  immunohistochemistry in AD and aACD and PPAR- $\gamma$  antagonism in skin T<sub>H</sub> cell lines.  
 Fig. S12. Gating strategies for flow cytometry analysis.  
 Table S1. Raw data file.  
 Table S2. Antibodies used in this study.  
 Table S3. RT-PCR primers used in this study.

### REFERENCES AND NOTES

1. F. Sallusto, A. Lanzavecchia, Heterogeneity of CD4<sup>+</sup> memory T cells: Functional modules for tailored immunity. *Eur. J. Immunol.* **39**, 2076–2082 (2009).
2. S. F. Ziegler, Division of labour by CD4<sup>+</sup> T helper cells. *Nat. Rev. Immunol.* **16**, 403 (2016).
3. V. Dardalhon, A. Awasthi, H. Kwon, G. Galileos, W. Gao, R. A. Sobel, M. Mitsdoerffer, T. B. Strom, W. Elyaman, I.-C. Ho, S. Khoury, M. Oukka, V. K. Kuchroo, IL-4 inhibits TGF- $\beta$ -induced Foxp3<sup>+</sup> T cells and, together with TGF- $\beta$ , generates IL-9<sup>+</sup> IL-10<sup>+</sup> Foxp3<sup>+</sup> effector T cells. *Nat. Immunol.* **9**, 1347–1355 (2008).
4. M. Veldhoen, C. Uytenhove, J. van Snick, H. Helmbly, A. Westendorf, J. Buer, B. Martin, C. Wilhelm, B. Stockinger, Transforming growth factor- $\beta$  'reprograms' the differentiation of T helper 2 cells and promotes an interleukin 9-producing subset. *Nat. Immunol.* **9**, 1341–1346 (2008).
5. S. Agarwal, A. Rao, Modulation of chromatin structure regulates cytokine gene expression during T cell differentiation. *Immunity* **9**, 765–775 (1998).
6. W. Zheng, R. A. Flavell, The transcription factor GATA-3 is necessary and sufficient for Th2 cytokine gene expression in CD4 T cells. *Cell* **89**, 587–596 (1997).
7. S. Becattini, D. Latorre, F. Mele, M. Foglierini, C. De Gregorio, A. Cassotta, B. Fernandez, S. Kelderman, T. N. Schumacher, D. Corti, A. Lanzavecchia, F. Sallusto, T cell immunity. Functional heterogeneity of human memory CD4<sup>+</sup> T cell clones primed by pathogens or vaccines. *Science* **347**, 400–406 (2015).
8. E. V. Acosta-Rodriguez, L. Rivino, J. Geginat, D. Jarrossay, M. Gattorno, A. Lanzavecchia, F. Sallusto, G. Napolitani, Surface phenotype and antigenic specificity of human interleukin 17-producing T helper memory cells. *Nat. Immunol.* **8**, 639–646 (2007).
9. C. Schlapbach, A. Gehad, C. Yang, R. Watanabe, E. Guenova, J. E. Teague, L. Campbell, N. Yawalkar, T. S. Kupper, R. A. Clark, Human T<sub>H</sub>9 cells are skin-tropic and have autocrine and paracrine proinflammatory capacity. *Sci. Transl. Med.* **6**, 219ra8 (2014).
10. P. Licona-Limón, J. Henao-Mejía, A. U. Temann, N. Gagliani, I. Licona-Limón, H. Ishigame, L. Hao, D. B. R. Herbert, R. A. Flavell, Th9 cells drive host immunity against gastrointestinal worm infection. *Immunity* **39**, 744–757 (2013).
11. C. Tan, M. K. Aziz, J. D. Lovaas, B. P. Vistica, G. Shi, E. F. Wawrousek, I. Gery, Antigen-specific Th9 cells exhibit uniqueness in their kinetics of cytokine production and short retention at the inflammatory site. *J. Immunol.* **185**, 6795–6801 (2010).
12. A. C. Richard, C. Tan, E. T. Hawley, J. Gomez-Rodriguez, R. Goswami, X.-p. Yang, A. C. Cruz, P. Penumetcha, E. T. Hayes, M. Pelletier, O. Gabay, M. Walsh, J. R. Ferdinand, A. Keane-Myers, Y. Choi, J. J. O'Shea, A. Al-Shamkhani, M. H. Kaplan, I. Gery, R. M. Siegel, F. Meylan, The TNF-family ligand TL1A and its receptor DR3 promote T cell-mediated allergic immunopathology by enhancing differentiation and pathogenicity of IL-9-producing T cells. *J. Immunol.* **194**, 3567–3582 (2015).
13. S. Ying, Q. Meng, A. B. Kay, D. S. Robinson, Elevated expression of interleukin-9 mRNA in the bronchial mucosa of atopic asthmatics and allergen-induced cutaneous late-phase reaction: Relationships to eosinophils, mast cells and T lymphocytes. *Clin. Exp. Allergy* **32**, 866–871 (2002).
14. N. Gulati, M. Suarez-Fariñas, J. Fuentes-Duculan, P. Gilleaudeau, M. Sullivan-Whalen, J. Correa da Rosa, I. Cueto, H. Mitsui, J. G. Krueger, Molecular characterization of human skin response to diphenylprone at peak and resolution phases: Therapeutic insights. *J. Invest. Dermatol.* **134**, 2531–2540 (2014).
15. M. H. Kaplan, M. M. Hufford, M. R. Olson, The development and in vivo function of T helper 9 cells. *Nat. Rev. Immunol.* **15**, 295–307 (2015).
16. R. A. Clark, C. Schlapbach, T<sub>H</sub>9 cells in skin disorders. *Semin. Immunopathol.* **39**, 47–54 (2017).
17. M. T. Wong, D. E. H. Ong, F. S. H. Lim, K. W. W. Teng, N. McGovern, S. Narayanan, W. Q. Ho, D. Cerny, H. K. K. Tan, R. Anicete, B. K. Tan, T. K. H. Lim, C. Y. Chan, P. C. Cheow, S. Y. Lee, A. Takano, E. H. Tan, J. K. C. Tam, E. Y. Tan, J. K. Y. Chan, K. Fink, A. Bertoletti, F. Ginhoux, M. A. Curotto de Lafaille, E. W. Newell, A high-dimensional atlas of human t cell diversity reveals tissue-specific trafficking and cytokine signatures. *Immunity* **45**, 442–456 (2016).

18. J. Gomez-Rodriguez, F. Meylan, R. Handon, E. T. Hayes, S. M. Anderson, M. R. Kirby, R. M. Siegel, P. L. Schwartzberg, Itk is required for Th9 differentiation via TCR-mediated induction of IL-2 and IRF4. *Nat. Commun.* **7**, 10857 (2016).
19. R. Jabeen, R. Goswami, O. Awe, A. Kulkarni, E. T. Nguyen, A. Attenasio, D. Walsh, M. R. Olson, M. H. Kim, R. S. Tepper, J. Sun, C. H. Kim, E. J. Taparowsky, B. Zhou, M. H. Kaplan, Th9 cell development requires a BATF-regulated transcriptional network. *J. Clin. Invest.* **123**, 4641–4653 (2013).
20. S. P. Nobs, S. Natali, L. Pohlmeier, K. Okreglicka, C. Schneider, M. Kurrer, F. Sallusto, M. Kopf, PPAR $\gamma$  in dendritic cells and T cells drives pathogenic type-2 effector responses in lung inflammation. *J. Exp. Med.* **214**, 3015–3035 (2017).
21. T. Chen, C. A. Tibbitt, X. Feng, J. M. Stark, L. Rohrbach, L. Rausch, S. K. Sedimbi, M. C. I. Karlsson, B. N. Lambrecht, G. B. Karlsson Hedestam, R. W. Hendriks, B. J. Chambers, S. Nylen, J. M. Coquet, PPAR $\gamma$  promotes type 2 immune responses in allergy and nematode infection. *Sci. Immunol.* **2**, eaal5196 (2017).
22. O. Gaide, R. O. Emerson, X. Jiang, N. Gulati, S. Nizza, C. Desmarais, H. Robins, J. G. Krueger, R. A. Clark, T. S. Kupper, Common clonal origin of central and resident memory T cells following skin immunization. *Nat. Med.* **21**, 647–653 (2015).
23. N. Sopol, A. Graser, S. Mousset, S. Finotto, The transcription factor BATF modulates cytokine-mediated responses in T cells. *Cytokine Growth Factor Rev.* **30**, 39–45 (2016).
24. P. Li, R. Spolski, W. Liao, W. J. Leonard, Complex interactions of transcription factors in mediating cytokine biology in T cells. *Immunol. Rev.* **261**, 141–156 (2014).
25. M. H. Kaplan, The transcription factor network in Th9 cells. *Semin. Immunopathol.* **39**, 11–20 (2017).
26. V. Popp, K. Gerlach, S. Mott, A. Turowska, H. Garn, R. Atreya, H. A. Lehr, I. C. Ho, H. Renz, B. Weigmann, M. F. Neurath, Rectal delivery of a DNazyme that specifically blocks the transcription factor GATA3 and reduces colitis in mice. *Gastroenterology* **152**, 176–192.e5 (2017).
27. K. Gerlach, Y. Y. Hwang, A. Nikolaev, R. Atreya, H. Dornhoff, S. Steiner, H.-A. Lehr, S. Wirtz, M. Vieth, A. Waisman, F. Rosenbauer, A. N. J. McKenzie, B. Weigmann, M. F. Neurath, T<sub>H</sub>9 cells that express the transcription factor PU.1 drive T cell-mediated colitis via IL-9 receptor signaling in intestinal epithelial cells. *Nat. Immunol.* **15**, 676–686 (2014).
28. S. Koch, N. Sopol, S. Finotto, Th9 and other IL-9-producing cells in allergic asthma. *Semin. Immunopathol.* **39**, 55–68 (2017).
29. D. Shik, S. Tomar, J.-B. Lee, C.-Y. Chen, A. Smith, Y.-H. Wang, IL-9-producing cells in the development of IgE-mediated food allergy. *Semin. Immunopathol.* **39**, 69–77 (2017).
30. B. Weigmann, M. F. Neurath, Th9 cells in inflammatory bowel diseases. *Semin. Immunopathol.* **39**, 89–95 (2017).
31. W. Yao, Y. Zhang, R. Jabeen, E. T. Nguyen, D. S. Wilkes, R. S. Tepper, M. H. Kaplan, B. Zhou, Interleukin-9 is required for allergic airway inflammation mediated by the cytokine TSLP. *Immunity* **38**, 360–372 (2013).
32. D. R. Neill, A. N. McKenzie, TH9 cell generation. TH9: The latest addition to the expanding repertoire of IL-25 targets. *Immunol. Cell Biol.* **88**, 502–504 (2010).
33. E. Vivier, S. A. van de Pavert, M. D. Cooper, G. T. Belz, The evolution of innate lymphoid cells. *Nat. Immunol.* **17**, 790–794 (2016).
34. C. Wilhelm, K. Hirota, B. Stieglitz, J. Van Snick, M. Tolaini, K. Lahl, T. Sparwasser, H. Helmby, B. Stockinger, An IL-9 fate reporter demonstrates the induction of an innate IL-9 response in lung inflammation. *Nat. Immunol.* **12**, 1071–1077 (2011).
35. E. Wambre, V. Bajzik, J. H. DeLong, K. O'Brien, Q.-A. Nguyen, C. Speake, V. H. Gersuk, H. A. DeBerg, E. Whalen, C. Ni, M. Farrington, D. Jeong, D. Robinson, P. S. Linsley, B. P. Vickery, W. W. Kwok, A phenotypically and functionally distinct human T<sub>H</sub>2 cell subpopulation is associated with allergic disorders. *Sci. Transl. Med.* **9**, eaam9171 (2017).
36. C. O. Park, T. S. Kupper, The emerging role of resident memory T cells in protective immunity and inflammatory disease. *Nat. Med.* **21**, 688–697 (2015).
37. C. E. Zielinski, F. Mele, D. Aschenbrenner, D. Jarrossay, F. Ronchi, M. Gattorno, S. Monticelli, A. Lanzavecchia, F. Sallusto, Pathogen-induced human T<sub>H</sub>17 cells produce IFN- $\gamma$  or IL-10 and are regulated by IL-1 $\beta$ . *Nature* **484**, 514–518 (2012).
38. Y. Endo, C. Iwamura, M. Kuwahara, A. Suzuki, K. Sugaya, D. J. Tumes, K. Tokoyoda, H. Hosokawa, M. Yamashita, T. Nakayama, Eomesodermin controls interleukin-5 production in memory T helper 2 cells through inhibition of activity of the transcription factor GATA3. *Immunity* **35**, 733–745 (2011).
39. X. Jiang, X. Ye, W. Guo, H. Lu, Z. Gao, Inhibition of HDAC3 promotes ligand-independent PPAR $\gamma$  activation by protein acetylation. *J. Mol. Endocrinol.* **53**, 191–200 (2014).
40. H. E. Xu, Y. Li, Ligand-dependent and -independent regulation of PPAR gamma and orphan nuclear receptors. *Sci. Signal.* **1**, pe52 (2008).
41. A. Werman, A. Hollenberg, G. Solanes, C. Bjorbaek, A. J. Vidal-Puig, J. S. Flier, Ligand-independent activation domain in the N terminus of peroxisome proliferator-activated receptor gamma (PPAR $\gamma$ ). Differential activity of PPAR $\gamma$ 1 and -2 isoforms and influence of insulin. *J. Biol. Chem.* **272**, 20230–20235 (1997).
42. T. S. Hughes, P. K. Giri, I. M. S. de Vera, D. P. Marciano, D. S. Kuruvilla, Y. Shin, A.-L. Blayo, T. M. Kamenecka, T. P. Burris, P. R. Griffin, D. J. Kojetin, An alternate binding site for PPAR $\gamma$  ligands. *Nat. Commun.* **5**, 3571 (2014).
43. K. Man, A. Kallies, Synchronizing transcriptional control of T cell metabolism and function. *Nat. Rev. Immunol.* **15**, 574–584 (2015).
44. J. D. Johansen, K. Aalto-Korte, T. Agner, K. E. Andersen, A. Bircher, M. Bruze, A. Cannavo, A. Gimenez-Arnau, M. Goncalo, A. Goossens, S. M. John, C. Liden, M. Lindberg, V. Mahler, M. Matura, T. Rustemeyer, J. Serup, R. Spiewak, J. P. Thyssen, M. Vigan, I. R. White, M. Wilkinson, W. Uter, European society of contact dermatitis guideline for diagnostic patch testing - recommendations on best practice. *Contact Dermatitis* **73**, 195–221 (2015).

**Acknowledgments:** We thank R. Jaggi, M. Fragnière, S. Schenk, and the genomics core facility of the Department of Clinical Research of the University of Bern for technical support. We are grateful to J. Stein, C. Conrad, and L. Michalik for helpful comments. **Funding:** This study was supported by the Peter Hans Hofschneider Professorship for Molecular Medicine, the Promedica Foundation, the W. & H. Berger-Janser Foundation, the Olga Mayenfisch Foundation, the Novartis Foundation for Biomedical Research, the Bernese League against Cancer, and the Inselspital CTU grants (all to C. Schlapbach); the Hans Stettler Foundation (to N.Y.); and the Swiss National Science Foundation (SNF project PP00P3\_163961; to B.S.). **Author contributions:** C.M., L.v.M., O.S., E.K., C.A., M.S., C.C., D.Y., and C. Schlapbach designed and performed the experiments. N.Y., D.S., L.B., S.K., B.H., C.C., and C. Schlapbach provided important reagents and funding. C. Simillion, S.M.S.J., P.O., B.S., and C. Schlapbach analyzed the data. C.M. and C. Schlapbach wrote the paper. **Competing interests:** The authors declare that they have no competing interests. **Data and materials availability:** The RNA-seq data are deposited on ArrayExpress (accession no. E-MTAB-5739).

Submitted 17 March 2018  
Accepted 26 November 2018  
Published 18 January 2019  
10.1126/sciimmunol.aat5943

**Citation:** C. Micossé, L. von Meyenn, O. Steck, E. Kipfer, C. Adam, C. Simillion, S. Morteza Seyed Jafari, P. Olah, N. Yawalkar, D. Simon, L. Borradori, S. Kuchen, D. Yerly, B. Homey, C. Conrad, B. Sniijder, M. Schmidt, C. Schlapbach, Human “T<sub>H</sub>9” cells are a subpopulation of PPAR- $\gamma$ <sup>+</sup> T<sub>H</sub>2 cells. *Sci. Immunol.* **4**, eaat5943 (2019).

## Human "T<sub>H</sub>9" cells are a subpopulation of PPAR- $\gamma$ <sup>+</sup> T<sub>H</sub>2 cells

Claire Micossé, Leonhard von Meyenn, Oliver Steck, Enja Kipfer, Christian Adam, Cedric Simillion, S. Morteza Seyed Jafari, Peter Olah, Nikhil Yawlkar, Dagmar Simon, Luca Borradori, Stefan Kuchen, Daniel Yerly, Bernhard Homey, Curdin Conrad, Berend Snijder, Marc Schmidt and Christoph Schlapbach

*Sci. Immunol.* 4, eaat5943.

DOI: 10.1126/sciimmunol.aat5943

### Licensing interleukin-9 production

Whereas the biological roles of T helper 1 (T<sub>H</sub>1), T<sub>H</sub>2, and T<sub>H</sub>17 cells are reasonably well established, the functions of interleukin-9 (IL-9)-secreting T<sub>H</sub>9 cells remains elusive. Several studies have documented the presence of T<sub>H</sub>9 cells in both humans and mice. Here, by studying human T<sub>H</sub> cells *ex vivo*, Micossé *et al.* propose that T<sub>H</sub>9 cells are a subpopulation of T<sub>H</sub>2 cells that transiently up-regulate IL-9 and report the transcription factor peroxisome proliferator-activated receptor- $\gamma$  (PPAR- $\gamma$ ) to be a key regulator of IL-9 production. The results presented by Micossé *et al.* call for a closer examination of the ontogeny of IL-9-producing T<sub>H</sub> cells using cytokine reporter mouse strains.

#### ARTICLE TOOLS

<http://immunology.sciencemag.org/content/4/31/eaat5943>

#### SUPPLEMENTARY MATERIALS

<http://immunology.sciencemag.org/content/suppl/2019/01/14/4.31.eaat5943.DC1>

#### REFERENCES

This article cites 44 articles, 10 of which you can access for free  
<http://immunology.sciencemag.org/content/4/31/eaat5943#BIBL>

Use of this article is subject to the [Terms of Service](#)